Accepted Manuscript

The coupling of Indian subduction and Asian continental tectonics

Anne Replumaz, Fabio A. Capitanio, Stéphane Guillot, Ana M. Negredo, Antonio Villaseñor

PII: S1342-937X(14)00104-X
DOI: doi: 10.1016/j.gr.2014.04.003
Reference: GR 1246

To appear in: *Gondwana Research*

Received date: 3 October 2013
Revised date: 7 April 2014
Accepted date: 11 April 2014

Please cite this article as: Replumaz, Anne, Capitanio, Fabio A., Guillot, Stéphane, Negredo, Ana M., Villaseñor, Antonio, The coupling of Indian subduction and Asian continental tectonics, *Gondwana Research* (2014), doi: 10.1016/j.gr.2014.04.003

Invited GR Focus Review

The coupling of Indian subduction and Asian continental tectonics

Anne Replumaz[1*], Fabio A. Capitanio[2], Stéphane Guillot[1], Ana M. Negredo[3], and Antonio Villaseñor[4]

[1] ISTerre, Université de Grenoble-Alpes, CNRS, 38041 Grenoble, France

[*] corresponding author, anne.replumaz@ujf-grenoble.fr

[2] School of Geosciences, Monash University, Clayton, Victoria 3800, Australia

[3] Dept. of Geophysics, Facultad CC. Físicas, Universidad Complutense de Madrid. Av. Complutense, 28040 Madrid. Spain.

[4] Instituto de Ciencias de la Tierra Jaume Almera, CSIC, Sole´ i Sabarı´s s/n, 08028 Barcelona, Spain

Abstract

In order to understand the potential controls on Asian tectonics during the subduction of the Tethys and Indian lithospheres, we reconstruct the coupled subduction-continent deformation history using tomographic imaging, kinematics constraints and numerical modeling.

The global P-waves tomographic images of the mantle below the India-Asia collision zone provide constraints on the deep structure of continents and subduction history. Linking the slab positions in the mantle to the Asian tectonics reconstructions and the Indian plate kinematics, we reconstruct the timing and location of successive subduction and breakoff events, showing one major breakoff occurred between India and the Tethys Ocean ~45 Ma. In the western syntax, a vertical slab continuous to the continent is shown to override the deeper detached Tethys slab. In the central region similar structure is found with a detached slab, yet closer to the Tethys slab. In the eastern syntax, no slab is imaged. It is inferred that after Tethys slab had broke off, subduction only resumed in the center of the margin, while underthrusting took place at both extremities of the convergent margin. During following convergence, a second breakoff event detached the central Indian slab from the margin ~15 Ma ago, which renewed Indian lithosphere underthrusting below Asia. This most probably occurred when the Tibetan Plateau was already uplifted, implying that uplift is not a direct result of underthrusting.

Numerical models of breakoff during subduction illustrate the controls of slab detachment on the complexities of the Indian margin. In these models the subduction of continental lithosphere resumes after breakoff only where this is entrained by the mantle flow associated with the long lasting oceanic slab sinking, that is in the centre of the margin, while converging continent edges underthrusts the upper plate. Furthermore, the breakoff during subduction has profound implications on the Asian intra-plate tectonics. In the models, the breakoff is rapidly followed by large stresses in the upper plate interiors, propagating at large distance from the margin, along a belt oriented at ~45˚ from the trench. The long-term evolution of the Asian continental tectonics shows drastic changes in the fault pattern, with successive strike-slip faulting across the Asian continent, which are in agreement with the mechanisms illustrated by the models. Transient large coupling at the trench caused by the breakoff events during India-Asia convergence offers an explanation for episodic nucleation of lithospheric faults within the Asian continent and their link to deep processes.

1. Introduction

Since almost one century, field observations in Tibet have been interpreted to infer the deep structure of the India/Asia collision zone, and to constrain models of continental deformation during collision. The first model by Emile Argand in 1924 proposed that the Indian continent stamps the Asian one and slides below it, uplifting the Tibetan Plateau (Argand, 1924). Since then, a large amount of data has been collected, that has revealed many complexities in the system and has led to controversial interpretations. Numerous analog and numerical models have been proposed, but no consensus has been reached upon the behavior of the continental lithosphere leading to the Tibetan Plateau formation (figure 1).

One kind of models focuses on the uniform altitude of the Plateau (Fielding et al., 1994). Analog models using silicone, and numerical models of viscous continental lithosphere successfully reproduce a viscous uniform thickening migrating northward of the Asian continent due to its indentation by the Indian continent (e.g. England and Molnar, 1997), or a uniform thickening of only the lower crust (Royden et al., 2008). The deformation of such viscous lithospheres has been successfully coupled to the subduction process in a Newtonian viscous mantle (e.g. Funicello et al., 2003). The subduction of the Indian continent, pulled down in the mantle by the still attached Tethys oceanic slab has been simulated unless India is scraped off its upper crust and part of its lower crust (Capitanio et al., 2010). The subduction in these conditions generates the advance of the trench and the indentation of the upper plate, which thickens and spreads laterally homogeneously (Bajolet et al., 2013).

Another kind of model focuses on the large thrusts observed in the Himalaya and the Tibetan Plateau, and the large strike-slip faults in Tibet. Analog models using sand, and numerical models of elasto-plastic continental lithosphere have successfully reproduced the building of a wedge with periodic localized thrusts thickening the crust, over a subduction zone, like observed in the Himalaya, or over a wide sub-horizontal intracrustal decollement, like the Northern Tibet's (e.g. Malavieille, 1984; Smit et al., 2003; Buiter et al., 2006). Analog models using plasticine, of plastic continental lithosphere have succeeded to reproduce wide strike-slip faults crossing the whole Asian continent, allowing for large horizontal motion of continental blocks. Yet, they do not address the thickening of Tibet, prevented by a glass on top of the plasticine (Peltzer and Tapponnier, 1988). Multi-layered sand-silicone (rigid/ductile) models of the crust generate strike-slip faults and thrusts, either homogeneously distributed or localized depending on the brittle-to-ductile strength ratio, but do not generate large horizontal motion nor reproduce northward propagation of thickening, which is instead occurring only in front of the indenter (Schueller and Davy, 2008). No numerical model has addressed the large strike-slip faulting accommodating hundreds of kilometers of displacement along thousands of kilometers long fault zones, due to the localization and high amplitude of the deformation on a very thin zone compared to a wide continent. To date, few models have explored the link between such intra-continental strike-slip faulting and the subduction process (Capitanio and Replumaz, 2013; Li et al., 2013).

Models have inferred different implications on the deep structure of the collision zone (e.g. Willett and Beaumont, 1994; Johnson, 2002). The global P-waves tomographic images of the mantle below the collision zone have been intensely used during the last 15 years to constrain such deep structure. Positive P-wave anomalies have been interpreted as mapping the slab position below the collision zone, which has been useful to constrain the subduction history of the Tethys ocean and northern part of Indian plate (van der Voo et al., 1999; Hafkenscheid et al., 2006; Negredo et al., 2007; Replumaz et al., 2010a; Li et al., 2008). The interpretations have been used to constrain models of continental subduction and breakoff (e.g. Wortel and Spakman, 2000; Negredo et al., 2007; Capitanio et al., 2010). Yet, the interactions between the continental subducting plate and the upper plate deformation during the collision between Asia and India have been relatively less investigated. In this paper, we relate the deep tomographic observations to Asian tectonics reconstructions (Replumaz and Tapponnier, 2003) and Indian plate kinematics (Patriat and Achache, 1984). On the basis of recent numerical models (Capitanio and Replumaz, 2013), we discuss the evolution of the Asian tectonics as the result of the upper plate coupling with the Indian subduction during the collision period.

2. Tomography constraints on subduction and breakoff

2.1. Mantle structure

High wavespeed anomalies are commonly interpreted as remnants of slabs, with deeper anomalies representing older subduction events (e.g. van der Hilst et al., 1997; Bijwaard et al., 1998; van der Meer et al., 2010). We use the P-waves global tomographic model of Bijwaard et al. (1998) to elucidate the 3D mantle seismic structure beneath the collision zone (figure 2). This model has been updated by Villaseñor et al. (2003) by including arrival times of earthquakes from 1995 to 2002 listed in the bulletins of the International Seismological Centre and reprocessed using the EHB methodology (Engdahl et al., 1998). Synthetic checkerboard tests estimate the resolving power of the travel time dataset at different depths (Replumaz et al., 2010b) showing that the size and location of the anomalies interpreted in this study are sufficiently well resolved. However, travel time tomography is known to show a vertical smearing and a partial loss of visibility of slabs as they penetrate into the lower mantle, as well as underestimating the seismic velocity anomaly values (e.g. van der Hilst, 1995; Bijwaard et al., 1998; Ricard et al., 2005). Therefore, for the interpretations in this study we will rely on the geometry of the high-velocity seismic anomalies, and not account for their amplitudes.

Several high wavespeed anomalies are observed beneath the collision zone (figures 2 and 3). The long high wavespeed anomaly labeled as TH trends NW–SE and appears laterally continuous along the entire plate boundary from at least 1600 km to 1100 km depths. Above the TH anomaly and north of it, there are several distinct high wavespeed anomalies labeled as IN, HK, BU, AN, PA, TI and AS. These anomalies appear laterally unconnected, suggesting a complex subduction history during India/Asia collision, with succession of subduction and breakoff events (Chemenda et al., 2000). The position and geometry of the significant anomalies shown in different P-waves tomographic models are very similar (Van der Voo et al., 1999; Replumaz et al., 2004; Hafkenscheid et al., 2006; Negredo et al., 2007; Richards et al., 2007; Li et al., 2008). Considering no stagnation of the slabs in the mantle, the P-waves positive anomaly depth can be related to the timing of subduction events. Under the assumption that lateral advection during subduction is negligible, the positive anomaly position indicates the approximate location where the slab impinged into the mantle, showing the position of the trench. Therefore the position and depth of the mantle P-waves positive anomalies have been correlated to the Indian plate kinematics reconstruction and to the Asian tectonics reconstruction, to infer the complex subduction history during India/Asia collision. We review in the following sections the timing of different subduction episodes beneath the collision zone (Replumaz et al., 2004, 2010a&b, 2013; Negredo et al., 2007), using the Indian plate kinematics of Patriat and Achache (1984), and the Asian tectonics reconstructions of Replumaz and Tapponnier (2003). We compare our results with other reconstructions leading to a different timing of events (e.g. Stampfli and Borel, 2002; van Hinsbergen et al., 2011).

2.2. Upper mantle positive anomalies related to on-going subductions, HK, PA, BU

High wavespeed anomalies labeled as HK, PA and BU, are related to on-going continental subduction underlined by seismicity describing a well-defined Wadati-Benioff zone down to the fragile/ductile transition depth, shallower than the tomographic slab image (Negredo et al., 2007).

The HK anomaly (beneath Hindu Kush) occurs from the surface down to 600 km depth, with a very steep geometry, underlined by seismicity down to 300 km, by far the most active area of intermediate-depth intracontinental seismicity (figure 3a). This deep seismicity has been first interpreted as an indication for the subduction of a trapped oceanic basin, based on seismological arguments (Chatelain et al., 1980). But considering that there has not been oceanic crust in the entire area of the western syntaxis since the Late Cretaceous, it is now widely accepted that the deep seismicity and the corresponding tomographic anomaly HK indicates the ongoing subduction of the Indian continental lithosphere under the Hindu Kush mountains (figures 3a and 5a) (e.g. Burtman and Molnar, 1993; Guillot et al., 2003; Koulakov and Sobolev, 2006; Negredo et al., 2007). To the south, the HK anomaly is in continuity with the anomaly labeled CR, related to the thick Indian craton (horizontal section at 200 km depth in Figure 2).

The anomaly PA (beneath PAmir) dips southward with a shallower dip than HK anomaly. It is observed from the surface down to 400 km depth and is underlined by seismicity down to 200 km (figure 3b). This anomaly has been interpreted as the ongoing subducting Asian lithosphere under the Pamir range (e.g. Burtman and Molnar, 1993; Fan et al., 1994; Negredo et al., 2007; Mechie et al., 2012; Sippl et al., 2013).

The BU anomaly (beneath Burma) is related to the ongoing eastward subduction of a microplate (Ni et al., 1989; Li et al., 2008), reaching a depth of about 400 km, with seismicity down to 200 km depth. Due to the direction of subduction perpendicular to the convergence, this anomaly has been interpreted as a piece of Indian lithosphere pushed eastward during the extrusion of Indochina, then subducted parallel to the eastern Indian plate boundary (figure 2; Replumaz et al., 2010a). The AN anomaly (beneath Andaman) is found between 300 and 600 km depth, and is curved below Andaman and northern Sumatra. It has been related to an early episode of southeastward extrusion followed by subduction, similar to the one related to the BU anomaly (figure 2; Replumaz et al., 2010a).

2.3. Lithospheric structure, comparing global tomography and seismic profiles

Beneath India, the P-waves tomographic cross-sections show a strong positive anomaly (+2-3%), marking the thick and cold lithospheric mantle of the Indian craton (anomaly labelled CR, figure 3). Such anomaly extends mostly flat beneath Tibet, instead it connects to deeper vertical anomalies beneath the Hindu Kush and central Tibet (figure 3a&f). Elsewhere, the CR positive anomaly starts dipping northward south of the Tsangpo suture to become flat lying northward (figure 3). P-waves global tomography provides constraints to the northern limit of the Indian continent below Tibet (Li et al., 2008; De Celles et al., 2002; Replumaz et al., 2013). To the west of the Tibetan Plateau, the CR positive deep anomaly reaches the Tarim basin, whereas it extends beneath the Bangong suture in the central Tibet, and beneath the Tsangpo suture in eastern Tibet. The northern extent of the CR anomaly also constrains the amount of Indian lithosphere underthrusting beneath Asia, which is largest in the west and decreases eastward (figure 3).

Beneath Tibet, global tomography has been compared to seismic profile obtained using the receiver function method, enhancing converted S waves from P waves of distant earthquakes impinging on interfaces beneath the recording stations (e.g. Li et al., 2008; Replumaz et al., 2013). Such methods give very accurate depth of interfaces down to ~150km, while global tomography shows the lateral and vertical continuity of lithospheric blocks at greater depth.

Along the TIPAGE profile beneath Pamir, the Indian Moho remains flat at shallow depth, reaching the area of deep crustal seismicity related to the southward subduction of Asian lithosphere beneath Pamir (Mechie et al., 2012; Sippl et al., 2013). The CR anomaly has a similar geometry (figure 3b).

Along the Hi-Climb seismic profile at longitude ~85°E, the Indian Moho bends south of the Tsangpo suture and continues flat-lying (Nabelek et al., 2009). The Moho is duplicated from the Tsangpo suture to 31°N latitude, and has been related to the top and bottom of the Indian lower crust which eclogitized during bending (Hetenyi et al., 2007). Nabelek et al.

(2009) interpreted the Indian Plate to extend as far north as 31°N, where the double Moho vanishes into a single interface lying between 60 and 70 km depth, north of 31°N, and inferred to be the Tibetan Moho. The positive anomaly related to the Indian Craton (CR) bends consistently with this seismic profile, but continues horizontally north of the Bangong suture to 34°N, farther than inferred from the Hi-Climb seismic profile (figure 5d) (De Celles et al., 2002; Replumaz et al., 2013).

Along the Indepth profile at longitude ~90°E, the existence of a south dipping interface has been revealed, interpreted as a steep subduction of the Asian Lithospheric Mantle extending to ~300 km (ALM; Kind et al., 2002) or as a shallower Asian Lithospheric Mantle extending only down to ~150 km (Yue et al., 2012), facing the northward subduction of the Indian lithospheric mantle (Tilmann et al., 2003; Yue et al., 2012). Both slabs have been observed in the P-wave tomography used here. The plunging CR positive anomaly in this area is consistent with the Indian lithospheric mantle interface (Figure 3f&g) (Li et al., 2008; Replumaz et al., 2013). The plunging TI positive anomaly is compatible with a flat Asian Lithospheric Mantle, observed only down to 200 km (Figure 5f&g), consistent with Yue and co-authors conclusions (Yue et al., 2012), and with the interpretation of De Celles and co-authors (De Celles et al., 2002). Less agreement is found in local tomography, with no positive anomaly corresponding to the ALM interface (Liang et al., 2012).

2.4. positive anomaly across the transition zone, IN: Indian continental slab?

The IN anomaly (beneath INdia) extends between ~900 km up to ~500 km depth, with a vertical extent increasing from west to east and a pronounced dip southward (figure 3c and d). It is the most prominent anomaly observed at intermediate mantle depths (figure 2), and is clearly visible on the different P-waves tomographic models, with variable geometry depending on the velocity anomaly amplitude chosen to contour (e.g. van der Voo et al., 1999 (named II anomaly); Hafkenscheid et al., 2006 (named Hi); Li et al., 2008 (named C); Replumaz et al., 2010 (named IN); van Hinsbergen et al., 2012 (named GIB)). However, the interpretation of this anomaly is the most controversial, with the nature of the subducted lithosphere, whether oceanic or continental, being matter of debate.

Our interpretation is that the IN anomaly corresponds to a slab of continental lithosphere, related to the subduction of a large portion of the northwestern margin of India (Replumaz et al., 2010b), in agreement with the interpretation of De Celles and co-authors (De Celles et al., 2002). Then, the length of the Indian continent is the addition of the length of the shallow horizontal anomaly related to the thick Indian craton (CR anomaly), stopping less than 500 km north of the Tsangpo suture, and the length of the IN anomaly (figures 3b-d). This length of the Indian continent is similar to length of the slab observed beneath the Hindu Kush, continuous down to 600 km depth (figure 3a), and comparable to the size of the Indian continent deduced from its original position in Gondwana, constrained between the Australian and Antartica continents (Gibbons et al., 2012; Zahirovic et al., 2012). By comparing the position of the IN anomaly with the position of India through time (Patriat and Achache, 1984), we estimated that the subduction process responsible for the anomaly IN initiated at 35±5 Ma (Replumaz et al., 2010b). It ended with a progressive slab break-off process (figure 5c) that started most probably around 25 Ma at the western end of the slab, where the slab length is short (figure 3b), and propagated eastwards, where the slab length is longer (figure 3c&d), until complete break-off around 15 Ma. The breakoff has been correlated with high-grade metamorphism from 28–15 Ma in the gneiss domes in north Himalaya and in the Pamir (Stearns et al., 2013). The IN anomaly is located north of the Asian margin at the onset of collision reconstructs by Replumaz and Tapponnier (2003). According to our interpretation, it is related to a subduction event during the indentation of Asia, beginning at ~45Ma.

The other interpretation is that the IN anomaly corresponds to a slab of oceanic lithosphere (e.g. van der Voo et al., 1999; Hafkenscheid et al., 2006; van Hinsbergen et al., 2012; Zahirovic et al., 2012), related to the subduction of the Spongtang oceanic back-arc basin, located between the Neo-Tethys and Eurasian continental margin (Stampfli and Borel, 2002). Such interpretation and the related paleogeographic reconstruction imply a much younger collision time that could be as young as ~20 Ma, occurring after the subduction of the oceanic back-arc basin, which has a shape corresponding fortuitously to the shape of the Indian indenter (figure 4).

2.5. Lower mantle positive anomaly below 1100 km, TH: Tethys Ocean slab

The high wavespeed anomaly TH observed beneath India from depths of ~1100 km down to at least 1600 km has been related to the continuous subduction of Tethys Ocean beneath Southeast Asia since at least the Cretaceous (Van der Voo et al., 1999; Replumaz et al., 2004; Hafkenscheid et al., 2006; Negredo et al., 2007; Richards et al., 2007). The TH anomaly vanishes at depths shallower that ~1100 km (figure 2), where vertical continuity between positive high wavespeed anomalies at shallower depths and the TH anomaly lacks (Figure 3). This is inferred to be a slab break-off.

The outline of the TH anomaly at this depth allows tracing the likely location and morphology of the northern boundary of India at the time of break-off (Negredo et al., 2007).

We constrained the size of the Indian continent after breakoff by the length of the Indian slab as it is presently subducting beneath the Hindu Kush (figure 3a). The absence of positive anomaly in between HK and TH (located about 10º south of HK) at this longitude shows that no subduction occurrred during the time elapsed between slab breakoff and the onset of subduction responsible for HK anomaly. The inferred contour outlining the Indian continent at the time of the break-off has been drawn accordingly (figure 4). Our estimate is remarkably similar to the size and shape of the Greater Indian continent deduced from its original position in Gondwana, located between the Australian and Antartica continents (Gibbons et al., 2012; Zahirovic et al., 2012). A wide greater India geometry (e.g. van Hinsbergen et al., 2011) is not compatible with such Gondwana geometry, and implies that the breakoff detached a large part of the northern boundary of such wide continent.

The match of paleogeographic Indian position and TH anomaly position, provides a relative estimate of the time of break-off. By using the paleo-position of India by Patriat and Achache (1984), which is very robust, Negredo and co-authors (2007) estimated an age of break-off between 44 and 48 Ma, when the convergence rate dropped drastically. The uncertainty is due to the width of the positive anomaly, a breakoff at 44 Ma fits the northern outline of the anomaly, while a break-off at 48 Ma fits the southern outline of the anomaly (figure 4). Paleogeographic reconstruction of Müller and co-authors (2008) shows a more progressive drop between 50 and 40 Ma, in agreement with a break-off age between 45 and 40 Ma, compatible with our timing. Reconstructions with a slower drop of the Indian velocity (drop between 50 and 30 Ma, break-off age between 40 and 35 Ma (van Hinsbergen et al., 2011); drop between 70 and 20 Ma, break-off age between 25 and 20 Ma (Molnar and Stock, 2009)) lead to a more recent collision, in disagreement with onset of continental volcanism and continental sedimentation observed in southern Tibet (Ding et al., 2007; Najman et al., 2010).

Under the assumption that lateral advection during subduction is negligible, the TH anomaly at 1100 km depth indicates the location where Tethys lithosphere impinged in the mantle. According to this interpretation, the TH anomaly indicates the position of the trench before the collision. This location is consistent with the last stage of the Asian tectonic reconstruction of Replumaz and Tapponnier (2003; see paragraph 3), which provides a relevant constraint on the position and geometry of the Asian upper plate convergent margin.

In the lower mantle, the TH anomaly extends to the east, around South-East Asia. To the east, the slab is continuous to the surface and no breakoff occurs (figure 2). In the upper mantle, a continuous positive anomaly follows the oceanic trench around Southeast Asia, marking the Indian oceanic slab (figure 2). This geometry drastically changes at depth, showing a linear structure beneath 1000 km. The change in the oceanic slab contours has been interpreted as matching the progressive deformation of Asia's margin, including India's indentation and Indochina's extrusion moving about 700 km eastward (Replumaz et al., 2004; Hall et al., 2008).

2.6. Lower mantle positive anomaly north of TH, AS: Asian slab?

Between 1100 and 900 km depth, north of and parallel to the TH anomaly, the low amplitude high-wavespeed anomaly AS has a length of ~3000 km (figure 2). It is a weak anomaly observed in the lower mantle, visible on different P-waves tomographic models (e.g. Hafkenscheid et al., 2006 (named PT); Replumaz et al., 2010c (named AS)).

Assuming no stagnation of the slabs in the mantle, its elongated geometry, running rather parallel to the plate boundary at the onset of collision, underlined by the TH anomaly located further south, suggests that this anomaly is the remnant of an episode of Asian continental subduction post-dating the OCT break-off event (Replumaz et al., 2013). The AS anomaly has been correlated with volcanism dated between 45 and 30 Ma located between the Jinsha and the Bangong sutures (Ding et al., 2007; Guillot and Replumaz, 2013). It could be equivalent to an Asian slab as present-day observed beneath Pamir (Figure 3b), detached from the continent and sinking into the lower mantle (figure 5). Considering a long stagnation of this slab at shallow depth, Hafkenscheid and co-authors (2006) interpreted this positive anomaly as an oceanic slab corresponding to the PaleoTethys slab (PT anomaly) in between Asian continental blocks, subducted long before the collision, but detached from the continent only between 80 and 60 Ma and since then sinking in the mantle.

3. Asian tectonics constraints on the over-riding plate deformations

The deformation of the Indian crust is to the first order that of a crustal wedge over a subducting lithosphere (e.g. Lavé and Avouac, 2000; Johnson, 2002). Such a crustal wedge is composed of successive thrusts rooting on an intra-crustal sub-horizontal decollement, the Main Himalayan Thrust, which thickened the entire brittle upper crust and part of the lower crust, forming the Himalaya range (Bollinger et al., 2006). It has been successfully reproduced by numerical and analogue experiments by the shortening of a sand layer above a sliding flat surface, mimicking lithospheric subduction (e.g. Malavieille, 1984; Smit et al., 2003; Buiter et al., 2008). However, the deformation of the Asian continent is more complex and extends over a much wider zone, making the intra-continental tectonics here unique. Because of the large and long-lasting deformation within the Asian continent the geometry of the Asian margin prior to collision is not easily inferred from its present-day shape. A first estimate is provided by the matching of the present-day geometry and the indentation-related structures, allow inferring a linear geometry between Sumatra and the mouth of Indus (Tapponnier et al., 1986; Le Pichon et al., 1992). More recently, the Asian margin geometry has been inferred from reconstructions of the Asian continent deformation. We synthetize here the data used and the results of the first complete reconstruction done (Replumaz and Tapponnier, 2003). By comparing this reconstruction at different time steps with tomographic sections at different depths, we constrain the major events in relation to the deep lithospheric processes (figure 6). We also constrain the initial geometry of the Asian margin and compare it with other studies (figure 4) (Royden et al., 2008; van Hinsbergen et al., 2011).

3.1. Asian tectonic reconstruction

The first time steps of the backward in time reconstruction of Replumaz and Tapponnier (2003) restore the present-day thickening of Tibet, occurring to the north of the Plateau (figure 6a). The northernmost thrusts in the Qilian Shan are active since at least 10Ma (Fang et al., 2004; Hetzel et al., 2013), earlier than previously estimated by Metivier et al. (1998). The thrusts in the north of the Plateau are branching on the Altyn Tagh fault (Meyer et al., 1998). This strike-slip fault runs on thousands of km, bounding the Tarim basin (figure 1). It extends on the entire lithosphere thickness (Wittlinger et al., 1998) and eases the eastward sliding of the North China block shown by GPS results (e.g. Zhang et al., 2004). From present-day to 15 Ma, the deformation is very similar (figure 6a), with migration of the deformation to the north of the Tibetan Plateau, along successive parallel faults, which propagate to the north along the Altyn Tagh fault (Metivier et al., 1998; Meyer et al., 1998; Liu-Zeng et al., 2008).

The active fault network changes drastically before 15 Ma (figure 6b). From approximately 15 to 30Ma, the deformation is driven by the eastward extrusion of the Indochina block, sliding along the Red River fault (RRF) (Tapponnier et al., 1986; Peltzer and Tapponnier, 1988) for 700+/-200 km (Leloup et al., 2001). Such large motion has opened the South China Sea pull-apart basin, at the eastern end of the Red River fault. The magnetic anomalies of the South China Sea show that the basin opened between 32 and 16 Ma and constrain the rotation pole of the Indochina peninsula during this period (Briais et al., 1993). This pole is key to this reconstruction, as it constrains the position of Indochina before extrusion, representing the eastern boundary of the collision zone (figure 6b). Additional motion occurred along the Red River fault between 40 and 30 Ma, closing smaller pull-apart basins as observed in the Tonkin Gulf (Replumaz et al., 2001), and in SE Asia (e.g. Hall et al., 2008). It anneals the total offset along the Red River Fault (Leloup et al., 2001), and restores the linearity of the eastern coast (figure 6c). More eastward motion occurs along faults present-day located south of Indochina, the Wang Chao and 3 pagodas faults (WF and PF, figure 1; Lacassin et al., 1997, 1998). The restoration of the thickening in Tibet also anneals the curvature of the Bangong and Jinsha sutures around the eastern syntaxis, and makes them in continuity with the Red River fault (figure 6c).

Before 40 Ma, the motions were confined to the front of the indenter, and directed northward (figure 6d). The eastern boundary of the deformed zone was most probably the Dien Bien Phu fault, connecting with the Ranong fault in Malaysia (DF and RF, figure 1). West of this fault, the Indochina crust was thickened, while east of the fault the crust was little affected by thickening. This eastern boundary was preserved for further deformation as the Indochina block was extruded eastward. The western boundary of this frontal deformation zone is less clear, as it has been over-printed by intense thickening in the following indentation process. The northern boundary of this early frontal deformation zone has been suggested to be localized along the Bangong suture (Replumaz and Tapponnier, 2003). Yet the volcanism dated between 45 and 30 Ma located between the Bangong and the Jinsha sutures (figure 1) has been considered as an evidence of early deformation north of the Bangong suture, related to early Asian continental subduction (Ding et al., 2007; Guillot and Replumaz, 2013).

The last stage of the reconstruction provides a relevant constraint on the position and geometry of the upper plate of the Asian convergent margin (figure 6e). It also matches the position and geometry of the Tethys trench at the onset of indentation, deduced from the position of the TH anomaly at depth, providing a coherent geometry of both continents in contact at the beginning of the indentation (figure 4).

One key constrain of this reconstruction is the position of the Indochina block at the onset of the collision, constraining the eastern boundary of the collision zone and the amount of shortening in central Tibet. A large motion along the Red River fault (700+/-200 km; Leloup et al., 2001; Briais et al., 1993), anneals the offset of the eastern Asian coast, the eastern syntaxis deformation around the Indian indenter corner and implies a large amount of shortening in central Tibet, by inserting the Indochina peninsula in its middle (figure 6d). By considering a similar amount of motion along the Red River fault, the schematic reconstruction of Royden and co-authors restores a similar geometry of the eastern Asian margin prior to collision, but a more oblique trench corresponding to a dissymmetric shape of India (Royden et al., 2008). Such trench is not corresponding to the TH anomaly geometry (figure 4). By considering a much smaller amount of motion along the Red River fault (250 km), the reconstruction of van Hinsbergen and co-authors shows an eastern Asian coast with a residual offset along the Red River fault, a residual curvature of the eastern syntaxis deformation and a smaller amount of shortening in central Tibet (van Hinsbergen et al., 2012). The resulting southern Asian margin shows a residual indentation mark, corresponding to the inferred shape of the Indian indenter, which does not align with the TH anomaly geometry (figure 4). Such reconstruction is compatible with the paleogeographic reconstruction of Stampfli and Borel, (2002), where an oceanic back-arc basin is located between the Neo-Tethys and Eurasian continental margin.

3.2. Asian crustal mass budget

The consistency of the reconstructed Asian margin geometry can be checked through a comparison with a first order budget of the Asian crust. The inferred crustal mass of the Asian continent at the onset of collision has been compared with the present-day mass, after the Asian continent has been thickened and its contour modified during the collision (figure 7). The present-day Asian crustal volume has been measured by adding the volume between the Moho (Villasenor et al., 2001) and the topographic surface north of the Tsangpo suture, except below 60 km depth where Indian crust underthrusts Asia (Nabelek et al., 2009; Mechie et al., 2012), and the volume of erosion (Metivier et al., 1999), multiplied by a mean crustal density of 2700 kg/m^3, using a simplified depth/density profile (Replumaz et al., 2010c). This present-day measured Asian crustal mass has been restored over the Asian continent area at the onset of the collision (figure 7). The obtained thickness represents the crustal mass that has been stored within the thickened crust or redistributed by extrusion, but spared from subduction and not recycled in the mantle. For the Asian continent, the estimated crustal thickness accommodated during collision is about 32 km. This value is close to a standard initial Asian crustal thickness, similar to what present-day observed for the Indochina peninsula, not affected by the thickening (figure 1). It is in agreement with an Asian continent not thickened before indentation, as presently observed along the Southeast Asian margin (figure 1).

Albeit simplified, the crustal balance shows that only a negligible amount of the Asian crust that has been recycled into the mantle (figure 7). It is in agreement with the inferred limited amount of Asian lithospheric mantle slabs, related to the AS and PA anomalies (figure 5). This suggests that the Asian crust has been either deformed by lateral motions along strike-slip faults, absorbing about 30% of the convergence (Replumaz & Tapponnier, 2003), or by crustal thickening, yet preserved from recycling in the mantle.

Such crustal budget is dependent upon the geometry and the mean altitude of the Asian continent at the onset of collision, leading to a non-unique interpretation. Alternatively, a reduced area of the Asian continent at the onset of collision (figure 4) (Stampfli and Borel, 2002; van Hinsbergen et al., 2012) but with a thick Asian crust before indentation similar to the Andean Plateau (Kapp et al., 2007), should also be compatible with such a crustal budget.

4. Numerical models constraints on subducting-upper plates interactions

Global tomography has revealed a complex Indian slabs geometry, corresponding to successive episodes of subduction and breakoff (figures 2&3). The Indian continental lithosphere has subducted down to the lower mantle, detached from the dense oceanic Tethys slab (figure 5). This interpretation is consistent with models showing than the recovered continental lithospheric buoyancy can drive subduction, thus no attached dense oceanic slab (Capitanio et al., 2010). To model the Indian continent subduction during the collision, one has to take into account the breakoff process, which separates the deep oceanic Tethys slab from the Indian continental plate. The rupture mechanics has been extensively studied in the last decades. Such rupture has been shown to occur at the OCT (Chemenda et al., 2000; Regard et al., 2005), caused by an excess of tensile stress during the bending due to the deep oceanic slab pull (e.g. Wong A Ton and Wortel, 1997; Duretz et al., 2012), and by thermal weakening (Gerya et al., 2004). Geophysical observable implication of such rupture has been quantified, as dynamic topography (Buiter et al., 2002). Lateral propagation of slab detachment likely occurs by stress focusing on the rupture tip, triggering further rupture (Yoshioka and Wortel, 1995; Wortel and Spakman, 2000), which can reach very high rates (Burkett and Billen, 2010; van Hunen and Allen, 2011).

In this paper, we do not address the details of rupture mechanics and we focus on the implications of slab loss. The rupture is modeled by varying the yield strength of the subducted oceanic plate, leading to spontaneous localization of large stresses and rupturing at the OCT. Here, we summarize the outcomes of recent numerical modeling that addressed the role of slab breakoff on continental subduction (Capitanio and Replumaz, 2013), as revealed by tomography analysis (figure 5). We show the link between such deep processes and continental tectonics during convergence, especially the drastic changes in the fault network shown by kinematic reconstruction of the Asian tectonics (Replumaz and Tapponnier, 2003).

4.1. Modelling approach

Subduction is modeled as the viscous Stokes flow of an infinite Prandtl number fluid and very low Reynolds number, neglecting the effect of temperature. Under these approximations, the force balance is governed by the conservation of mass, enforcing the incompressibility condition, and momentum equations. Linearised rheological profiles are used for the plates and the mantle. To model the continental lithosphere, we used a parameterised slab buoyancy variation (Capitanio et al., 2010), and do not vary the rheology of the plates. Thus, continental subduction is modeled as the entrainment of the lighter plate following a denser one.

The ambient mantle is a Newtonian fluid of viscosity 2.10^{20} Pa s. The subducting lithosphere has a 70 km thick top layer with a viscosity 1000 times larger than the mantle viscosity, and a 30 km thick bottom layer with a viscosity 10 times larger and a composite visco-plastic rheology. The subducting plate-mantle density contrast is 80 kg m^{-3} for the oceanic domain, and is reduced to 1/3 in the continental domains. The resulting integrated buoyancy values are compatible with that of continental lithospheres with an eclogitic/amphibolitic crust (Cloos, 1993). The upper plate has no density contrast with the mantle, and is fixed in the far-field. It has either a Newtonian viscosity 1000 or 100 times larger that the mantle, or a composite visco-plastic rheology to address the role of upper plate deformation during convergence.

The rupture in the slab is induced by reducing locally the plate's plastic limit. The rupture occurs at the OCT, where spontaneous localization of large stresses occurs (Wong A Ton and Wortel, 1997). For the yield strength chosen, the breakoff occurs at a depth of ~100 km, when the tensile stresses are maximised (Duretz et al., 2012). The width of the slab detachment is either limited to a portion of the slab or the slab is completely removed.

We solve equations in their non-dimensionalised form using a Particle-in-cell finite element method, Underworld, where Lagrangian integration points (40 particles/element) are embedded in a three-dimensional Eulerian mesh of 96x96x64 elements (Moresi et al., 2003; Stegman et al., 2006).

4.2. Complete and partial slab breakoff

In the simple models where subduction is ongoing, the oceanic slab eventually extends to the base of the upper mantle. In this steady-state subduction stage the slab accumulates atop the upper-lower mantle boundary. This is then perturbed by continental plate subduction, which is entrained into the mantle and eventually subducting at smaller rates.

When a partial breakoff occurs at the OCT, the continental lithosphere still attached to the oceanic slab follows subduction, while where it is detached, the deep oceanic slab sinks and splits from the stalled continental slab above the breakoff.

Slab deformation accommodates the different dips along the trench. For the reduced continental buoyancy, the integrated pull of the stalled continental slab tip above the breakoff is not enough to drive self-sustaining subduction and lower plate remains at shallow depths, underthrusting the overriding lithosphere (figure 8). The detached tip of the lithosphere has progressively overridden both the detached deeper slab and the position of the original trench, whereas laterally, the slab is continuous. At surface, the subduction margin bends, with increasing curvature with convergence (figure 8), as the underthrusting stalled tip further separates from the subducting margin. The underthrusting is rather independent on the modality of breakoff, either instantaneous or propagating, and on the upper plate rheology, which is shown to only affect the curvature (Capitanio and Replumaz, 2013).

With a total slab break-off at the OCT, the subduction evolution of the continental plate is very similar (figure 8). The breakoff affects the continuity of the slab but not the poloidal mantle flow in the center of the slab, where the vertical convective cell extends throughout the upper mantle (figure 9). Although the slab vertical continuity is lost, stresses still propagate from the sinking slab to surface through the mantle viscous coupling. Instead, at the slab edge, the toroidal flow does not effectively drag the shallow lithospheric tip into the mantle (Funicello et al., 2003). Above the slab breakoff, the downgoing plate is dragged to the convergent margin by lateral stress propagated through the plate, resulting in the indentation of the upper plate (figure 9).

The most striking difference between partial and complete breakoff is the drop in the velocity of convergence (figure 9). The occurrence of partial breakoff does not change much the velocity evolution of the entrainment of continental slabs, as large pull is still applied through the lithospheric slab. The driving force progressively reduces as lighter lithosphere arrives to the trench and the convergence rate decreases to stabilize to a lower value as sustained continental subduction occurs. With the continental buoyancy drop tested, the subduction rate decreases to ~1 cm/yr within ~30 Ma. With a complete breakoff, the convergence rate drops much more rapidly (< 5 Ma) with all the continental buoyancies tested, to reach the same lower terminal velocity of the partial breakoff model of ~1 cm/yr.

4.3. Localized upper plate stresses due to breakoff

The coupling between the upper plate and the subducting slabs occurs through shear traction propagated by the ambient mantle, where flow is sustained by the downgoing slab (Capitanio et al., 2010; Capitanio et al., 2011). One striking result is that the upper plate stresses are rather small and diffuse in the models with a coherent slab at depth, and are instead large and strongly localised in the upper plate interiors when breakoff occurs (Capitanio and Replumaz, 2013). In the models with a coherent slab, shearing at the interplate boundary accommodates the stress at surface. No localisation is observed within the upper plate, and the stress measured is representative of an average over the whole upper plate. Instead, in the models where the breakoff occurs, the distribution of the stress in the upper plate is strongly localised, increasing largely above the tip of the slab breakoff at depth. In this case, all the models show the same pattern of a stress belt propagating largely into the upper plate for ~1200 km at an angle with the trench of 45˚±5˚ (figure 8). This is the result of stress coupling gradients at the trench, which to the first order reflect the distribution of slab mass at depth, and are thus less dependent on the simplified rheologies used. Similar stress belt allowing for lateral extrusion has been modelled by Li et al. (2013).

The upper plate stress is transient and decays within ~5 Ma for the oceanic plate subduction and more slowly in the lighter continent, where stress can be large for ~10 Ma. Peak stresses rapidly increase as the subduction rates decrease. Following further entrainment of less negatively buoyant continent, available pull forces progressively decrease, and the upper plate stress decreases. Similar peak stresses are found in the complete slab breakoff model, where a rapid drop in the upper plate stresses follows the pull force removal, with a duration similar to the convergence rate drop, ~5 Ma. Then, the upper plate transition to low stress regime occurs almost instantaneously.

5. Discussion: Linking Asian tectonics to deep lithospheric processes

We further show here that the global P-waves tomographic images of the mantle below the collision zone are useful to constrain the deep structure of the continents and their subduction history. By linking the slab positions shown by tomography to Asian tectonic reconstructions (Replumaz and Tapponnier, 2003) and Indian plate kinematics (Patriat and Achache, 1984), we infer successive subduction and breakoff events, and give an estimate of the timing of these events (figure 5). Such temporal evolution of deep processes allows discriminating between different models of continental deformation during collision (e.g. Willett and Beaumont, 1994; Johnson, 2002). First, tomography shows that part of the lithosphere of both continents has sunk into the mantle during the collision process, thus ruling out the occurrence of homogeneous thickening of both lithospheric mantle and crust (e.g. England and Molnar, 1997). Second, seismic tomography illustrates a discontinuous continental subduction process, with several breakoffs occurring during collision. The major one most likely occurred at the OCT between India and the Tethys Ocean, at about 45 Ma, showing that India is not pulled into the mantle attached to the deeper denser Tethys slab, as considered in simplified models (e.g. Capitanio et al., 2010; Bajolet et al., 2013). The dynamics of the rupture has been extensively studied during the last 20 years (Yoshioka and Wortel, 1995; Wong A Ton and Wortel, 1997; Wortel and Spakman, 2000; Gerya et al., 2004; Buiter et al., 2002; Burkett and Billen, 2010; van Hunen and Allen, 2011; Duretz et al., 2012), but the implications of such deep rupture on the Asian tectonics has been only recently modelled (Capitanio and Replumaz, 2013; Li et al., 2013). Third, global P-waves tomography shows that the deep lithosphere evolution during the collision is very heterogeneous along the Himalayan range, in contrast with its relatively homogeneous surface shape. This shape, the curvature and syntaxis appearance, has been successfully reproduced by a continuous continental subduction of India (Bajolet et al., 2013), suggesting that deep breakoffs did not affect the building of the Himalayan shape. On the contrary the deep heterogeneous processes are likely relevant for the emergence of heterogeneous deformation style affecting the Asian tectonics as strike-slip faulting, underthrusting and resumed subduction (e.g. Peltzer and Tapponnier, 1988; Copley et al., 2011).

In this section we describe the different implications of the deep structure of the collision zone deduced from tomography, upon Indian lithospheric mantle mass budget, the timing and implications of the underthrusting of India below Tibet, the link between Indian slab breakoff and Asian lithosphere tectonics, the subduction of Asian lithospheric mantle, and the driving force of the collision.

5.1. Underthrusting of Indian lithosphere since Middle Miocene

Underthrusting of the Indian lithosphere beneath the entire Tibetan Plateau was the first mechanical process proposed to link the wide deformation of the Asian crust to deeper lithospheric processes (Argand, 1924). Global P-waves tomography and seismic profiles support the occurrence of underthrusting of the Indian continent beneath Asia, although this does not extend beneath the entire Tibetan Plateau. To the west of the collision zone, at 75°E longitude, the TIPAGE seismic profile shown that the Indian lithosphere is flat lying, and reaches Central Pamir (Mechie et al., 2012). Along the Hi-Climb profile at 85°E longitude, flat-lying Indian lithosphere is also imaged, extending to the Bangong suture in Central Tibet (Nabelek et al., 2009; Hetenyi et al., 2007). P-waves global tomography has been used to follow more continuously the northern limit of the Indian continent below Tibet (Figure 10) (Li et al., 2008; Replumaz et al., 2013). The thick Indian craton is clearly visible on tomographic sections as a ~200 km thick prominent positive anomaly (CR anomaly, figure 2). Beneath the Hindu Kush, the Indian lithosphere bends and subducts vertically (figure 3a), north of the Tsangpo suture, whereas it instead remains flat at shallow depth beneath Pamir (figure 3b), extending to the area of the deep crustal seismicity related to the southward subduction of Asian lithosphere (figure 10) (Mechie et al., 2012). Beneath Western Tibet, the Indian lithosphere remains flat at shallow depth (figure 3c) and reaches the thinner (~100 km) positive anomaly related to the Tarim craton, whereas beneath Central Tibet, the flat lying Indian lithosphere (figure 3d) reaches the Bangong suture (figure 10). Its northern limit has a sharp contrast with the negative velocity anomaly of the Tibetan lithosphere, which is related either to the presence of hydrated minerals (Billen and Gurnis, 2001) or to hotter temperature (Jiménez-Munt et al., 2008). To the east of the Tibetan Plateau, the Indian lithosphere northern limit is close to the Tsangpo suture (figure 3f and g), showing that little underthrusting occurs there (figure 10).

The northern extent of the Indian lithosphere beneath the Asian continent is shorter than the minimum size of the Indian continent prior to collision (dashed green line on figure 10 showing the size of the Indian continent at the time of the breakoff from Negredo et al. (2007), similar to the Indian shape deduced by Gibbons et al. (2012)). It implies that underthrusting is not the only way convergence has been accommodated since the beginning of the collision. The interpretation of tomographic cross-sections leads us to conclude that subduction of the Indian lithosphere occurred in the middle part of the northern margin of India at the beginning of the collision, then the slab break off occurred at 25-15 Ma and underthrusting began at about 15 Ma (figure 5).

The variation of the Indian lithospheric mantle northern limit from west to east of the collision zone contrasts with the continuity of the Tibetan Plateau (figure 1). The relatively homogeneous altitude of the Plateau is in contrast with underthrusting limited to the southern part. The underthrusting of the Indian plate below Asian lithosphere occurs late in the collision time, since middle Miocene (figure 5). It most probably began when the Plateau was already uplifted, which implies that the Tibetan uplift is not a direct result of Indian Plate underthrusting (Chemenda et al., 2000; DeCelles et al., 2002). Yet the northern edge of the Indian underthrusting has been considered to coincide with the limit between dominantly strike-slip faulting in northern Tibet and dominantly normal faulting in southern Tibet (Copley et al., 2011), which occurs at the Jiali fault zone running between the eastern and western Himalayan syntaxes (figure 1). This contrast in tectonic regime is not likely to be due to lateral variations in topographically induced stresses, given the uniform elevation of the plateau, and has been linked to underthrusting (figure 10). Where underthrusting occurs, to the south of the Tibetan Plateau, the Indian lower crust acts in a rigid manner, the surface motions are accommodated by the shearing of the upper crust over the rigid lower crust, so that the Asian lithosphere at the surface is mechanically coupled to the Indian one at depth, leading to east–west extension of the upper crust (Copley et al., 2011). Although the northern edge of the Indian underthrusting does not exactly coincide with the Jiali fault zone, as this fault is visible in the middle of the CR anomaly to the west, and far north of the anomaly to the east (figure 10), the overlapping of extension and underthrusting suggests that underthrusting could affect the tectonics of the Tibetan Plateau, since the Middle Miocene, even if it is not the main mechanism to build the Plateau.

5.2. Indian lithospheric mantle and crust mass budget

The area comprised between the Indian northern boundary at the time of the break-off and the present-day northern boundary of underthrusted India (figure 10), provides an estimate of the total amount of Indian lithosphere involved in the indentation process that was consumed by subduction or extrusion. The anomalies HK, IN, BU and AN have been interpreted as the result of successive continental subduction episodes, which successively removed a portion of the Indian lithosphere northern margin (Replumaz et al., 2010a). The HK and IN anomalies have been interpreted to represent the subducted Indian lithosphere to the west of the collision zone. The BU and AN anomalies, presently trending north-south along the eastern border of India, have been interpreted as portions of the Indian lithosphere initially located to the north of the Indian continent, and extruded to the east where they subducted. This balance shows that the continental subduction, the extrusion and underthrusting processes inferred from the analysis of tomographic anomalies, accommodated the entire lithosphere of the northern Indian margin since the onset of indentation (figure 11).

The geometry of the Indian continent at the onset of indentation has been inferred from the geometry of the lower mantle positive anomaly TH, and from the length of the present-day slab beneath the Hindu Kush (figure 4). The geometry of the Asian continents at the onset of indentation has been deduced from tectonic reconstruction (figure 6). It matches the position of the TH anomaly at depth (figure 4). The inferred area of the two continents at the onset of collision has been compared with their present-day crustal mass after they have been thickened and their contours modified during the collision (figure 7). The results have been presented for the Asian continent in section 3.2. For the Indian continent, we add the volume between the Moho and the topographic surface south of the Tsangpo suture, the volume below 60 km depth north of the suture, where Indian crust underthrusts Asia, and the volume of erosion, and we use a simplified depth/density profile to estimate the crustal mass (Replumaz et al., 2010c). This present-day measured crustal mass has been spread over the area of the blocks at the onset of the collision, which give the thickness of India that has been stored within the thickened crust, spared from subduction and not recycled in the mantle (figure 7). For the Indian continent, this spared thickness is ~22 km, about half of the present-day average crustal thickness of the Indian craton, ~38 km. It implies that 40% of Indian crust was recycled into the mantle by continental subduction, with a mean decoupling level at 15 km depth. This depth corresponds approximately to the present-day depth of the Main Himalayan Thrust underlying the Himalayan mountain belt (e.g., Schulte- Pelkum et al., 2005; Nabelek et al., 2009). This large estimated amount of crust that has been recycled in the mantle is in agreement with the large amount of Indian lithospheric mantle subducted, related to the anomalies HK, IN, BU and AN (figure 11), with a part of the lower crust attached (Johnson, 2002; Hetenyi et al., 2007).

On the contrary for the Asian continent, as already discussed in section 3.2, the crustal thickness preserved from subduction during collision is about 32 km. This value is in agreement with a standard Asian continent not thickened before indentation as observed present-day along the Southeast Asian margin (figure 1). It is in agreement with a negligible amount of the Asian crust recycled into the mantle (Sobel et al., 2013), corresponding to few Asian slabs inferred from tomography, related to the AS and PA anomalies (figure 11), and possibly a larger amount of underthrusting of Asian lithosphere beneath north and central Tibet (Guillot and Replumaz, 2013).

5.3. Breakoff and Asian Tectonics inception

The inception of Asian tectonics and its relation to subduction remain poorly understood (figure 6). The numerical models presented here support the idea that slab breakoff caused stress accumulation in the upper plate that potentially produced or reactivated lithospheric yielding along structure oriented at ~45˚ from the trench and intersecting it near the slab (figure 8).

The OCT breakoff is associated with a frontal deformation delimited by two faults departing at an angle of about 45° from both Indian continent edges, to the east the Dien Bien Phu fault connecting with the Ranong fault, to the northwest the Bangong suture reactivated (figure 6D). The geometry of the faults is compatible with the geometry of the stress accumulation in the upper plate due to slab breakoff, suggesting that breakoff could have caused the lithospheric yielding necessary to activate such discontinuities (figure 12). The breakoff probably initiated to the west and propagates to the east along the entire OCT.

After the onset of indentation, the reactivated Bangong suture, departing from the subducting trench located to the north of the Indian continent, accommodated the incipient Asian extrusion (figure 6C), thus relevant stress propagated to this area. The partial slab breakoff occurring as the slab related to anomaly IN subducted steeply beneath Central Tibet while the slab related to the anomaly HK underthrusted beneath western Tibet, could have provided the cause for the large coupling and activation of such fault (figure 12). Likely, the Bangong suture provided a weaker inherited heterogeneity allowing for the localization of strain.

The Altyn Tagh fault also departs from the subducting trench located to the north of the Indian continent, and accommodated the propagation of the Asian deformation towards the north-east (figure 6). Similarly to what discussed before, relevant stress had to propagate to this portion of the Asian plate and thus could have been consequences of the second slab breakoff occurring between 25 and 15 Ma (figure 12).

The stress accumulation in the upper plate that follows the slab breakoff potentially leads to or reactivate the lithospheric shearing at ~45˚ from the trench. This model is in agreement with the evolution of Asian tectonics, thus we infer that localized stress following breakoff provide a potential explanation for the inception of the Asian tectonics (figure 12).

5.4. Continental subduction of Asian lithospheric mantle

The subduction of the Asian continental lithosphere has been suggested to occur at depth as the overlying crust thickened (Mattaeur, 1984; Tapponnier et al., 2001). A clear evidence of such a process is given by the on-going subduction of the Asian lithosphere beneath the

Pamir (Chatelain et al., 1980; Burtman and Molnar, 1993; Fan et al., 1994; Negredo et al., 2007; Sobel et al., 2013; Mechie et al., 2012). This slab has a shallow dip, underlined by seismicity down to 200 km, and traced by tomography down to 400 km depth (figure 3b). Along the TIPAGE seismic profile at 75°E longitude, the Indian lithosphere underlies the Central Pamir, and reaches the deep crustal seismicity related to the Asian subduction (Mechie et al., 2012). Such geometry suggests the penetration of the Indian lithosphere in between the Asian crust and lithospheric mantle. This decoupling allows for the ablation of the Asian lithospheric mantle, which sinks in the mantle (Sobel et al., 2013). Such a process likely preserves the Asian crust from recycling, as supported by no crustal deficits in the Asian crustal mass balance. The AS anomaly is found north of and shallower than the TH anomaly related to the oceanic subduction of the Tethys, and beneath the Asian continent, thus suggests that this lithospheric slab likely belonged to the Asian continent and began to sink when Indian continental lithosphere impinged in the trench (Replumaz et al., 2010c, 2013). By combining tomographic sections with the Asian tectonic reconstruction, the position of the wide AS anomaly matches the reconstructed position of the Bangong and Jinsha sutures to the south of the collision zone at the onset of indentation (Figure 6d), and likely related to the subduction of Asian lithospheric mantle bending beneath the Jinsha suture and sinking below the Bangong suture (Guillot and Replumaz, 2013). This episode has been constrained by the widespread K-rich lavas and subordinate Na-rich basalts, consistent with a source derived from melting of enriched lithospheric mantle, dated between 45 and 33 Ma, located between the Bangong and the Jinsha sutures (Roger et al., 2000; Ding et al., 2007). A magmatic episode related to subduction between ~50 and ~40 Ma has been also described in Kohistan (Bouillol et al., 2013), which could also be associated with this episode.

In the present-day, the thickening of Tibet occurs in the Qilian Shan north of the Plateau (figure 1), along thrusts rooting on an intra-crustal decollement merging beneath the Kunlun range (Meyer et al., 1998; Liu-Zeng et al., 2008). It has been related to Asian lithosphere subduction beneath the Kunlun suture (Tapponnier et al., 2001), but no evidence of such slab is found in tomography. A subduction of Asian lithosphere plunging southwards down to about 300 km has been observed along the Indepth profile (Kind et al., 2002). Nevertheless, the lateral extend of this slab is reduced, less than 200 km (TI anomaly, figure 2; Replumaz et al., 2013), and cannot be considered as a major ongoing process. It has been proposed that present-day the Asian lithosphere is partly underthrusting the Asian crust (Guillot and Replumaz, 2013), as suggested by the shape of the negative tomographic anomaly, lying flat at shallow depth (figure 3f and g).

5.5 Tethys and Indian subduction as a driving force of indentation

The forces driving convergence during continental collision are not fully understood. The Indian continental lithosphere has long been considered too buoyant to actively drive subduction, and external forcing, as large-scale mantle flow or pull of neighbouring slabs has been invoked (Li et al., 2008; Alvarez, 2010; Capitanio et al., 2011; Becker and Facenna, 2011). Recent numerical models have shown that a continent lithosphere as the Indian one has the ability to subduct under its own pull, as it is separated from its upper crust and part of its lower crust (Capitanio et al., 2010). Continental subduction of such lithosphere reduces the convergence rate by a factor 3, similar to that observed for India-Asia relative motions (Guillot et al. 2003, Zahirovic et al., 2012, van Hinsbergen et al., 2011b, White and Lister, 2012), but still provides enough force to drive the convergence process. However, this model assumed that large stresses propagated from an oceanic slab to the sinking Indian lithosphere. The complex Indian slab geometry revealed by global tomography, with successive episodes of breakoff (figure 5), shows that the correlation between convergence and deep subduction is less simple. The model presented here shows than even after a partial or a complete break-off at the OCT, the mantle flow generated by the long lasting subduction of the Tethys ocean, and the deeper Tethys slab sinking into the mantle, is strong enough to allow Indian continent resuming subduction (figure 8, Capitanio and Replumaz, 2013; Li et al., 2013). This is in agreement with the force balance around the present-day Indian motion, which requires the propagation of stresses from deep mantle flow to the surface around the Indian slab (Becker and Faccenna, 2011).

The IN anomaly has been related to an early subduction episode of the Indian lithosphere, occurring soon after the break-off of the Tethys oceanic root, similar to the complete breakoff model presented here. The model-predicted terminal velocity of ~1 cm/yr after complete breakoff, is far lower than the velocity of the Indian plate. This requires external forcing to partially sustain convergence, as Indian Ocean ridge push, large-scale mantle flow active by that time, plume interactions or pull transmitted from neighbouring slabs (e.g. Li et al., 2008; Capitanio et al., 2010, van Hinsbergen et al., 2011, Becker and Faccenna, 2011).

The breakoff of the slab related to the IN anomaly at about 15 Ma represents the end of large scale subduction in the collision zone. The slab observed at 90°E along the Indepth profile (Kind et al., 2002), and along corresponding tomographic cross-section (Figure 3f; Li et al., 2008; Replumaz et al., 2013), still attached to the Indian craton, could correspond to a more recent episode of subduction assisted by the mantle flow generated by the subduction of the Indian lithosphere (figure 8). Nevertheless, the small lateral extend of this slab (less than 200 km), together with the absence of intermediate depth seismicity, suggest that present-day subduction of Indian lithosphere occurs only locally, and therefore plays a secondary role as a mechanism presently accommodating plate convergence.

6. Conclusion

We explore the coupling between the deep subduction of the Indian continent and the tectonics of the Asian continental upper plate interiors. The long-term evolution of both lithospheres during convergence has been deduced from remnants of slabs in the mantle shown by P-waves global tomography. Successive episodes of subduction and breakoff have been evidenced (figures 2&3). A complete breakoff most likely occurred at about 45 Ma at the transition between the Tethys Ocean and the Indian continent, detaching the Tethys slab, clearly visible in the lower mantle as a prominent positive anomaly (TH). According to us, this anomaly shows the position of the trench at the onset of collision, showing the northern boundary of the Indian continent after the OCT breakoff, and the southern Asian margin. Such margin is in agreement with the Asian tectonics reconstruction of Replumaz and Tapponnier (2003) showing a linear margin, not with reconstructions showing a complex margin (figure 4) (Royden et al., 2008; van Hinsbergen et al., 2011).

Subsequently the evolution of the Indian lithosphere varies with time and space (figure 5). To the west of the collision zone, tomographic cross-sections show a continuous vertical slab (HK), interpreted as the subduction of the Indian continent down to 600km depth, far north of the deep detached Tethys slab. It is facing a shallower Asian continental slab beneath Pamir (PA), in agreement with seismic profile (Mechie et al., 2012; Sippl et al., 2013). In the central region a prominent deep slab is detached from the continent (IN), and reaches north of, yet closer to, the detached Tethys slab. It used to be interpreted as an oceanic slab (van der Voo et al., 1999; Hafkenscheid et al., 2006; van Hinsbergen et al., 2012). According to us it is a piece of the Indian continent, allowing to reconstruct the shape of the Indian continent prior to the OCT breakoff (figure 4a), which is very similar to the shape of the Indian continent deduced from its original position in Gondwana (Gibbons et al., 2012; Zahirovic et al., 2012). To the east no slab is imaged in the upper mantle. It has been deduced that soon after the breakoff of the Tethys slab, the Indian plate resumed subduction in the central part of its northern margin, while underthrusting beneath Asia occurred at both extremities of the continent. In the following indentation process, a second slab breakoff process, ending at about 15 Ma, detached the central slab from the continent. It implies that the present-day underthrusting observed under South Tibet occurs late in the collision history, most probably when the Plateau was already uplifted. Thus the Tibetan uplift is unlikely a direct result of Indian Plate underthrusting (Chemenda et al., 2000; DeCelles et al., 2002), in agreement with the contrast between the homogeneous altitude of the Plateau and the limited amount of underthrusting, shown by the thick shallow positive anomaly (figure 10). Yet the overlapping of South Tibet extension and underthrusting (Copley et al., 2011) suggests that underthrusting could affect the tectonics of the Tibetan Plateau since the Middle Miocene, even if it is not the main mechanism to build the Plateau. To the west, subduction of the Indian plate resumed less than 10 Ma ago beneath the Hindu Kush (Negredo et al., 2007), while to the east pieces of the Indian northern margin were extruded eastward.

Crustal mass budget implies that almost half of the Indian crust has been recycled into the mantle during the successive episodes of continental subduction (figure 7), attached to the lithospheric mantle (Hetenyi et al., 2008). On the contrary, crustal mass budget suggests that the Asian crust has been mostly preserved from recycling in the mantle, and deformed either by horizontal motions along strike-slip faults or by crustal thickening, as shown beneath Pamir (Sobel et al., 2013).

Numerical models help exploring the dynamics of continental lithosphere subduction. After slab breakoff at the OCT, either partial or complete, the edge of the continent underthrusts the upper plate, while along the centre subduction resumes, entrained by the mantle flow generated by the long lasting subduction of the ocean (figure 9), and sustained by its own buoyancy, negative enough to resume subduction after breaking off. Numerical modeling results also show that slab breakoff is rapidly followed by large stresses in the upper plate interiors, propagating at large distance from the margin, which potentially produced or reactivated lithospheric yielding along structure oriented at ~45˚ from the trench and intersecting it near the slab (figure 8). The long-term evolution of the Asian continental tectonics show drastic changes in the fault pattern, with successive strike-slip faulting across the Asian continent, with a trend similar to model-predicted orientations. We propose that successive Indian slab breakoff episodes have resulted in successive localized stress pulses which provide the conditions for the formation of Central Asian intra-continental faults. Transient coupling gradients at the trench caused by the breakoff events during India-Asia convergence offer an explanation for episodic nucleation of lithospheric faults within the Asian continent and their link to deep processes (figure 12).

Acknowledgements

This work has been supported by a grant from Labex OSUG@2020 (Investissements d'avenir – ANR10 LABX56) and the ANR DSP-Tibet.

Tomographic images were made using the graphic program P developed by Wim Spakman.

References

Alvarez, W., 2010. Protracted continental collisions argue for continental plates driven by basal traction. Earth and Planetary Science Letters, 296, 434-442, doi:10.1016/j.epsl.2010.05.030

Argand, E., 1924. La tectonique de l'Asie, 13[ième] Congrès Géologique International, 171-372

Bajolet F., Replumaz A., Lainé R. , 2013, Orocline and syntaxes formation during subduction and collision, Tectonics, 32, 1–18, doi:10.1002/tect.20087

Becker, T. W., and Faccenna C., 2011. Mantle conveyor beneath the Tethyan collisional belt. Earth and Planetary Science Letters, 310, 453-461.

Bijwaard, H., Spakman, W., and Engdahl, E.R., 1998. Closing the gap between regional and global travel time tomography. Journal of Geophysical Research, 103, 30055-30078.

Billen, M. I. and Gurnis M., 2001. A low viscosity wedge in subduction zones. Earth and Planetary Science Letters, 193, 227-236, doi: 10.1016/S0012-821X(01)00482-4

Bollinger, L., Henry, P., and Avouac, JP, 2006. Mountain building in the Nepal Himalaya: Thermal and kinematic model. Earth and Planetary Science Letters, 244, 58-71, doi: 10.1016/j.epsl.2006.01.045

Bouilhol, P., Jagoutz O., Hanchar J.M. and Dudas F.O., 2013. Dating the India–Eurasia collision through arc magmatic records. Earth and Planetary Science Letters, 366, 163–175, doi: 10.1016/j.epsl.2013.01.023

Briais, A., Patriat, P., Tapponnier, P., 1993. Updated interpretation of magnetic-anomalies and sea-floor spreading stages in the South China Sea - Implications for the Tertiary tectonics of South-Asia. Journal of Geophysical Research, 98, 6299-6328, doi: 10.1029/92JB02280

Buiter, S. J. H., et al. (2002), Two-dimensional simulations of surface deformation caused by slab detachment, Tectonophysics, 354(3-4), 195-210.

Buiter, S. J. H., et al. (2006), The numerical sandbox: Comparison of model results for a shortening and an extension experiment, Book Series: Geological Society Special Publication, 253, p 29-64, DOI: 10.1144/GSL.SP.2006.253.01.02

Burkett, E. R., and M. I. Billen (2010), Three-dimensionality of slab detachment due to ridge–trench collision: laterally simultaneous boudinage versus tear propagation, Geochemistry Geophysics Geosysteme, 11, Q11012.

Burtman, V.S. and Molnar, P., 1993. Geological and geophysical evidence for deep subduction of continental crust beneath the Pamir. Spec.Pap.-Geol. Soc. Am. 281, p76

Capitanio, F.A., Morra, G., Goes, S., Weinberg, R.F., Moresi, L., 2010. India-Asia convergence driven by the subduction of the Greater Indian continent. Nature Geoscience, 3, 136–139, doi: 10.1038/NGEO725.

Capitanio, F. A., Faccenna C., Zlotnik S., Stegman D. R., 2011. Subduction dynamics and the origin of Andean orogeny and Bolivian Orocline, Nature, 480, 83-86, doi:10.1038/nature10596

Capitanio, F.A. and Replumaz A., 2013. Subduction and slab breakoff controls on Asian Indentation tectonics and Himalayan Western Syntaxis formation, Geochemistry Geophysics Geosysteme, doi: 10.1002/ggge.20171

Chemenda, A. I., Burg, J. P. and Mattauer, 2000. M. Evolutionary model of the Himalaya-Tibet system: geopoem based on new modelling, geological and geophysical data. Earth and Planetary Science Letters, 174, 397-409

Chatelain, J.L., Roecker, S.W., Hatzfeld, D., Molnar, P., 1980. Microearthquake seismicity and fault plane solutions in the HinduKush region and their tectonic implications. Journal of Geophysical Research, 85, 1365–1387.

Royden, L. H., B.C. Burchfiel, R.D. van der Hilst, (2008), The geological evolution of the Tibetan plateau, Science, 321, p1054-1058, DOI: 10.1126/science.1155371

Cloos, M., 1993. Lithospheric buoyancy and collisional orogenesis: Subduction of oceanic plateaus, continental margins, island arcs, spreading ridges, and seamounts, Geological Society of America Bulletin, 105, 715-737.

Copley, A., J.-P. Avouac, B. P.Wernicke (2011), Evidence for mechanical coupling and strong Indian lower crust beneath southern Tibet, Nature, 472, p. 79-81, DOI: 10.1038/nature09926

De Celles, P.G., Robinson, D.M., and Zandt, G., (2002). Implications of shortening in the Himalayan fold-thrust belt for uplift of the Tibetan Plateau. Tectonics, 21, doi:10.1029/2001tc001322

Ding, L., Kapp, P., Yue, Y. & Lai, Q., 2007. Postcollisional calc-alkaline lavas and xenoliths from the southern Qiangtang terrane, central Tibet, Earth and Planet Science Letters, 254, 28-38. E. R.

Duretz, T., S.M. Schmalholz and T.V. Gerya, 2012. Dynamics of slab detachment, Geochemistry Geophysics Geosysteme, 13, doi: 10.1029/2011GC004024

Engdahl, R. D. van der Hilst, R. P. Buland, 1998. Global teleseismic earthquake relocation with improved travel times and procedures for depth determination. Bulletin of the Seismological Society of America, 88, 722-743

England, P., and P. Molnar, The field of crustal velocity in Asia calculated from Quaternary rates of slip on faults, Geophysical Journal International, 130, 551-582, 1997.

Fan, G., Ni, J.F., Wallace, T.C., 1994. Active tectonics of the Pamirs and Karakorum. Journal of Geophysical Research, 99, 7131–7160.

Fang, X., Zhao, Z., Li, J., Yan, M., Pan, B., Song, C., Dai, S., 2004. Magnetostratigraphy of the late Cenozoic Laojunmiao anticline in the northern Qilian Mountains and its implications for the northern Tibetan Plateau uplift. Science in China, Series D: Earth Sciences 34, 97–106.

Fielding, E., B. Isacks, M. Barazangi et al., (1994), How flat is Tibet, Geology, 22, p. 163-167

Funiciello, F., C. Faccenna, D. Giardini, and K. Regenauer-Lieb (2003), Dynamics of retreating slabs: 2. Insights from three-dimensional laboratory experiments, Journal of Geophysical Research, 108(B4), 2207, doi:10.1029/2001jb000896.

Gerya, T. V., et al. (2004), Thermomechanical modeling of slab detachment, Earth and Planetary Science Letters, 226, 101-116.

Gibbons, A. D., Barckhausen U., van den Bogaard P., Hoernle K., Werner R., Whittaker J. M., and Müller R. D., 2012. Constraining the Jurassic extent of Greater India: Tectonic evolution of the West Australian margin, Geochemistry Geophysics Geosysteme, 13, Q05W13, doi:10.1029/2011GC003919

Guillot, S., Garzanti E., Baratoux D., Marquer D., Maheo G. and de Sigoyer J., 2003. Reconstructing the total shortening history of the NW Himalaya. Geochemistry Geophysics Geosysteme, 4, doi:10.1029/2002gc000484

Guillot S. and Replumaz A., 2013. Importance of continental subductions for the growth of the Tibetan plateau. Bulletin de la Société Géologique de France. 184, 197-221

Hafkenscheid, E., Wortel, M.J.R., and Spakman, W., 2006. Subduction history of the Tethyan region derived from seismic tomography and tectonic reconstructions. Journal of Geophysical Research, 111, doi:10.1029/2005jb003791

Hall, R., M.W.A. van Hattum and W. Spakman, 2008. Impact of India–Asia collision on SE Asia: The record in Borneo, Tectonophysics, 451, 366–389, doi:10.1016/j.tecto.2007.11.058

Hetenyi, G., Cattin, R., Brunet, F., Bollinger, L., Vergne, J., Nabelek, J. and Diament, M., 2007. Density distribution of the India plate beneath the Tibetan plateau: Geophysical and petrological constraints on the kinetics of lower-crustal eclogitization. Earth and Planetary Science Letters, 264, doi: 10.1016/j.epst.2007.09.036

Hetzel, R., 2013. Active faulting, mountain growth, and erosion at the margins of the Tibetan Plateau constrained by in situ-produced cosmogenic nuclides, Tectonophysics, 582, 1-24, doi: 10.1016/j.tecto.2012.10.027

Jimenez-Munt, I., Fernandez, M., Verges, J., Platt, J.P., 2008. Lithosphere structure underneath the Tibetan Plateau inferred from elevation, gravity and geoid anomalies. Earth and Planetary Science Letters, 267, 276–289. doi:10.1016/s0012-821x(04)00070-6.

Johnson, M.R.W., (2002), Shortening budgets and the role of continental subduction during the India–Asia collision, Earth-Science Reviews, 59, p 101–123,

Kapp, P., P.G. DeCelles, G.E. Gehrels, M. Heizler, and L. Ding (2007), Geological records of the Lhasa-Qiangtang and Indo-Asian collisions in the Nima area of central Tibet, Geological Society America Bulletin, 119, 917–932. DOI: 10.1130/B26033.1

Kind, R., Yuan, X., Saul, J., Nelson, D., Sobolev, S.V., Mechie, J., Zhao,W., Kosarev, G., Ni, J., Achauer, U., Jiang, M., 2002. Seismic images of crust and upper mantle beneath Tibet: evidence for Eurasian plate subduction. Science 298, 1219–1221.

Koulakov, I., and S. V. Sobolev, 2006. A tomographic image of Indian lithosphere break-off beneath the Pamir–Hindukush region. Geophysical Journal International, 164, 425-440.

Lacassin, R., H. Maluski, P. H. Leloup, P. Tapponnier, C. Hinthong, K. Siribahakdi, S. Chuaviroj, and A. Charoenravat, 1997. Tertiary diachronic extrusion and deformation of western Indochina: Structural and 40Ar/39Ar evidence from NW Thailand, Journal of Geophysical Research, 102, 10,013 – 10,037

Lacassin R., Replumaz A., Leloup H., 1998. Harpin river loops and slip sense inversion on south-east Asian strike-slip faults, Geology, v. 26, p. 703-706

Lavé, J., and J. P. Avouac, 2000. Active folding of fluvial terraces across the Siwaliks Hills, Himalaya of central Nepal, Journal of Geophysical Research, 105, 5735–5770

Leloup, P.H., Arnaud, N., Lacassin, R., Kienast, J. R., Harrison, T. M., Trong, T. T. P., Replumaz, A. and Tapponnier, P., 2001. New constraints on the structure, thermochronology, and timing of the Ailao Shan-Red River shear zone, SE Asia. Journal of Geophysical Research, 106, 6683-6732.

Le Pichon, X., M. Fournier, and L. Jolivet, Kinematics, topography, shortening, and extrusion in the India-Eurasia collision, Tectonics, 11, 1085-1098, 1992.

Li, C., R. D. van der Hilst, A. S. Meltzer and E. R. Engdahl, 2008. Subduction of the Indian lithosphere beneath the Tibetan Plateau and Burma. Earth and Planetary Science Letters, 274, doi:10.1016/j.epsl.2008.07.016

Li, Z., Xu, Z., Gerya, T., Burg, J.-P. (2013) Collision of continental corner from 3-D numerical modeling. Earth and Planetary Science Letters, 380, 98-111, doi:10.1016/j.epsl.2013.08.034

Liang, Xiaofeng; Sandvol, Eric; Chen, Y. John; et al. (2012) A complex Tibetan upper mantle: A fragmented Indian slab and no south-verging subduction of Eurasian lithosphere. Earth and Planetary Science Letters, 333, p101-111, doi:10.1016/j.epsl.2012.03.036

Liu-Zeng, J., P. Tapponnier, Y. Gaudemer and L. Ding, 2008. Quantifying landscape differences across the Tibetan plateau: Implications for topographic relief evolution, Journal of Geophysical Research, 113, DOI: 10.1029/2007JF000897

Malavieille, J., 1984, Modélisation expérimentale des chevauchements imbriqués: application aux chaînes de montagnes. Bulletin de la Société Géologique de France, 26, 129–138.

Mattauer, M., 1986. Intracontinental subduction, crust-mantle décollement and crustal-stacking wedge in the Himalayas and other collision belts. Geological Society of London Special Publication, 19, 37-50

Mechie, J., Yuan X., Schurr B., Schneider F., Sippl C., Ratschbacher L., Minaev V., Gadoev M., Oimahmadov I., Abdybachaev U., Moldobekov B., Orunbaev S. and Negmatullaev S., 2012. Crustal and uppermost mantle velocity structure along a profile across the Pamir and southern Tien Shan as derived from project TIPAGE wide-angle seismic data. Geophysical Journal International, 188, 385-407, doi: 10.1111/j.1365-246X.2011.05278.x

Metivier, F., Y. Gaudemer, P. Tapponnier, and B. Meyer, 1998. Northeastward growth of the Tibet plateau deduced from balanced reconstruction of two depositional areas: The Qaidam and Hexi Corridor basins, China, Tectonics, 17, 823– 842, doi:10.1029/98TC02764.

Metivier, F., Y. Gaudemer, P. Tapponnier, and M. Klein, 1999. Mass accumulation rates in Asia during the Cenozoic, Geophysical Journal International, 137, 280–318

Meyer, B., Tapponnier, P., Bourjot, L., Métivier, F., Gaudemer, Y., Peltzer, G., Guo, S. & Chen, Z., 1998. Crustal Thickening in Gansu-Qinghai, Lithospheric mantle subduction, and oblique, strike-slip controlled growth of the Tibet Plateau. Geophysical Journal International, 135, 1-47.

Molnar, P., and J. M. Stock, 2009. Slowing of India's convergence with Eurasia since 20 Ma and its implications for Tibetan mantle dynamics. Tectonics, 28, TC3001, doi:10.1029/2008TC002271.

Moresi, L., F. Dufour and H.B.Muhlhaus, 2003. A lagrangian integration point finite element method for large deformation modeling of viscoelastic geomaterials, Journal of Computional Physics, 184, 476-497, doi: 10.1016/S0021-9991(02)00031-1

Nábělek, J., Hetényi G., Vergne J., Sapkota S., Kafle B., Mei Jiang, Heping Su, John Chen, Bor-Shouh Huang and the Hi-CLIMB Team, 2009. Underplating in the Himalaya-Tibet Collision Zone Revealed by the Hi-CLIMB Experiment. Science, 325, doi:10.1126/science.1167719

Najman, Y., E. Appel , M. Boudagher-Fadel, P. Bown, A. Carter, E. Garzanti, L. Godin, Jingtai Han, U. Liebke, G. Oliver, R. Parrish and G. Vezzoli, 2010. Timing of India-Asia collision: Geological, biostratigraphic, and palaeomagnetic constraints, Journal of Geophysical Research, 115, DOI: 10.1029/2010JB007673

Negredo, A.M., Replumaz, A., Villaseñor, A., and Guillot, S., 2007. Modeling the evolution of continental subduction processes in the Pamir-Hindu Kush region. Earth and Planetary Science Letters, 259, doi:10.1016/j.epsl.2007.04.043

Ni, J.F., Guzman-Speziale, M., Bevis, M., Holt, W.E., Wallace, T.C., Seager, W., 1989. Accretionary tectonics of Burma and the three-dimensional geometry of the Burma subduction zone. Geology 17, 68–71

Patriat, Ph., Achache, J., 1984. India–Eurasia collision chronology has implications for crustal shortening and driving mechanisms of plates. Nature 311, 615–621.

Peltzer, G., and P. Tapponnier, 1988. Formation and evolution of strike-slip faults, rifts, and basins during India-Asia collision: An experimental approach, Journal of Geophysical Research, 93, 15,085– 15,117

Priestley, K., Debayle, E., McKenzie, D. & Pilidou, S. Upper mantle structure of eastern Asia from multimode surface waveform tomography. Journal of Geophysical Research, 111, doi:10.1029/2005jb004082 (2006).

Regard, V., C. Faccenna, J. Martinod and O. Bellier, 2005. Slab pull and indentation tectonics: insights from 3D laboratory experiments, Physics of the Earth and Planetary Interiors, 149, 99-113, doi:10.1016/j.pepi.2004.08.011

Replumaz, A., and Tapponnier, P., 2003. Reconstruction of the deformed collision zone between India and Asia by backward motion of lithospheric blocks. Journal of Geophysical Research, 108, doi:10.1029/2001jb000661

Replumaz A., Lacassin R., Tapponnier P. and Leloup, P. H., 2001. Plio-Quaternary slip rate along the Red River Fault deduced from long term river offsets, Journal of Geophysical Research, 108, 19-836,

Replumaz, A., Karason, H., van der Hilst, R.D., Besse, J. and Tapponnier, P., 2004. 4-D evolution of SE Asia's mantle from geological reconstructions and seismic tomography. Earth and Planetary Science Letters, 221, doi:10.1016/s0012-821x(04)00070-6

Replumaz, A., Negredo, A. M., Guillot, S. and Villaseñor, A., 2010a. Multiple episodes of continental subduction during India/Asia convergence: Insight from seismic tomography and tectonic reconstruction, Tectonophysics, doi:10.1016/j.tecto.2009.10.007

Replumaz, A. Negredo A.M., Villaseñor A. and Guillot S., 2010b. Indian continental subduction and slab break-off during Tertiary Collision, Terra Nova, 22, 290-296, doi: 10.1111/j.1365-3121.2010.00945.x

Replumaz, A. Negredo A.M., Guillot S., van der Beek P. and Villaseñor A., 2010c. Crustal mass budget and recycling during the India/Asia collision, Tectonophysics, 492, 99-107, doi: 10.1016/j.tecto.2009.10.007

Replumaz, A., Guillot, S., Villaseñor, A. and Negredo, A. M., 2013. Amount of Asian lithospheric mantle subducted during the India/Asia collision, Gondwana Research, 24, 936–945, doi : 10.1016/j.gr.2012.07.019

Ricard, Y., Mattern, E. & Matas, J. Synthetic tomographic images of slabs from mineral physics. Earth's Deep Mantle: Structure, Composition, and Evolution 160, 283-300 (2005).

Richards, S., Lister, G., and Kennett, B., 2007. A slab in depth: Three-dimensional geometry and evolution of the Indo-Australian plate. Geochemistry Geophysics Geosysteme, 8., doi:10.1029/2007gc001657

Roger F, Tapponnier P., Arnaud N., Scharer U., Brunel, Xu, ZQ and Yang, JS, 2000. An Eocene magmatic belt across central Tibet: mantle subduction triggered by the Indian collision?, Terra Nova, 12, p102-108 DOI: 10.1046/j.1365-3121.2000.00282.x

Schueller, S., and P. Davy (2008), Journal of Geophysical Research, 113, B12404, doi:10.1029/2007JB005560,

Schulte-Pelkum, V., Monsalve, G., Sheehan, A., Pandey, M.R., Sapkota, S., Bilham, R., and Wu, F., 2005. Imaging the Indian subcontinent beneath the Himalaya. Nature, 435, 1222-1225.

Smit, J. H. W., J. P. Brun, and D. Sokoutis, 2003. Deformation of brittle-ductile thrust wedges in experiments and nature, Journal of Geophysical Research, 108(B10), 2480, doi:10.1029/2002JB002190,.

Sobel, E. R., Jie Chen, L. M. Schoenbohm, R. Thiede, D. F. Stockli, M. Sudo, M. R. Strecker,, 2013. Oceanic-style subduction controls late Cenozoic deformation of the Northern Pamir orogeny, Earth and Planetary Science Letters, 363, 204–218, doi:10.1016/j.epsl.2012.12.009

Stampfli, G. M., and G. D. Borel (2002), A plate tectonic model for the Paleozoic and Mesozoic constrained by dynamic plate boundaries and restored synthetic oceanic isochrons, Earth and Planetary Science Letters, 196, 17–33.

Stearns, M.A., B.R. Hacker, L. Ratschbacher, J. Lee, J. M. Cottle and A. Kylander-Clark, 2013. Himalaya driven by plate-scale dynamics Synchronous Oligocene−Miocene metamorphism of the Pamir and the north, Geology, 41, 1071-1074, doi: 10.1130/G34451.1

Stegman, D. R., Freeman, J., Schellart, W.P., Moresi, L., May, D., 2006. Influence of trench width on subduction hinge retreat rates in 3-D models of slab rollback, Geochemistry Geophysics Geosysteme, 7, 1-22, doi:10.1029/2005GC001056

Tapponnier, P., and P. Molnar, 1976. Slip-line field theory and large-scale continental tectonics, Nature, 264, 319-324.

Tapponnier, P., Peltzer, G., Armijo, R., 1986. On the mechanics of the collision between India and Asia. In: Ramsay, J.G., Coward, M.P., Ries, A.C. (Eds.), Collision tectonics. : Geological Society of London Special Publication, 19, pp. 115–157.

Tapponnier, P., Xu, Z.Q., Roger, F., Meyer, B., Arnaud, N., Wittlinger, G. and Yang, J. S., 2001. Oblique stepwise rise and growth of the Tibet plateau. Science, 294, 1671-1677.

van der Hilst, R.D., Widiyantoro, S., and Engdahl, E.R., (1997). Evidence for deep mantle circulation , Nature, 386, p 578-584

van der Meer, D.G., Spakman W., van Hinsbergen D.J.J., Amaru M.L. and Torsvik T.H., 2010. Towards absolute plate motions constrained by lower-mantle slab remnants: Nature Geoscience 3, 36 – 40, doi:10.1038/ngeo708

van der Voo, R., Spakman, W., and Bijwaard, H., 1999. Tethyan subducted slabs under India. Earth and Planetary Science Letters, 171, 7-20.

van Hinsbergen, D. J. J., P. Kapp, G. Dupont-Nivet, P. C. Lippert, P. G. DeCelles, and T. H. Torsvik, 2011. Restoration of Cenozoic deformation in Asia and the size of Greater India, Tectonics, 30, TC5003, doi:10.1029/2011TC002908.

van Hinsbergen D. J. J. et al., (2012), Greater India Basin hypothesis and a two-stage Cenozoic collision between India and Asia, Proceedings of the National Academy of Sciences, 109, doi/10.1073/pnas.1117262109

van Hunen, J., and M. B. Allen (2011), Continental collision and slab break-off: a comparison of 3D numerical models with observations, Earth and Planetary Science Letters, 302, 27-37.

Villaseñor, A., Ritzwoller, M.H., Levshin, A.L., Barmin, M. P., Engdahl, E. R., Spakman, W. and Trampert, J., 2001. Shear velocity structure of central Eurasia from inversion of surface wave velocities. Physics of the Earth and Planetary Interiors, 123, 169-184.

Villaseñor, A., Spakman, W. & Engdahl, E. R., 2003. Influence of regional travel times in global tomographic models, Geophysical Research Abstract, 5, abstr. EAE03-A-08614

Willett S.D. and C. Beaumont, (1994), Subduction of Asian lithospheric mantle beneath Tibet inferred from models of continental collision, Nature, 369, p 642-645

Wittlinger, G., Vergne, J., Tapponnier, P., Farra, V., Poupinet, G., Jiang, M., Su, H., Herquel, G. & Paul, A., 2004. Teleseismic imaging of subducting lithosphere and Moho offsets beneathy western Tibet. Earth and Planet Science Letters, 221, 117-130.

Wong A Ton, S. Y. M., and M. J. R. Wortel (1997), Slab detachment in continental collision zones: An analysis of controlling parameters, Geophysical Research Letter, 24(16), 2095-2098.

Wortel, M.J.R. and Spakman, W., 2000. Geophysics – subduction and slab detachment in the Mediterranean-Carpathian region. Science, 290, 1910–1917.

Yoshioka, S., and M. J. R. Wortel (1995), Three-dimensional numerical modeling of detachment of subducted lithosphere, Journal of Geophysical Research, 100(B10), 20223-20244.

Yue, H., Y. J. Chen, E. Sandvol, et al. (2012) Lithospheric and upper mantle structure of the northeastern Tibetan Plateau. Journal of Geophysical Research, 117, doi:10.1029/2011JB008545

Zahirovic, S., R. D. Müller, M. Seton, N. Flament, M. Gurnis, and J. Whittaker, 2012. Insights on the kinematics of the India-Eurasia collision from global geodynamic models. Geochemistry Geophysics Geosysteme, 13, Q04W11, doi:10.1029/2011GC003883.

Zhang, PZ, Z. Shen, M. Wang, et al., 2004. Continuous deformation of the Tibetan Plateau from global positioning system data. Geology, 32, 809–812, doi: 10.1130/G20554.1

Figure legend

Figure 1 : topographic map of the collision zone between India and Asia, showing faults (fine black lines; F fault; RRF: Red River; DF: DienBienPhu; WF: WangChao; PF: 3 Pagodas; RF: Ranong; SF: Sagaing; AT: Altyn Tagh; QSF: QilianShan; KuF: Kunlun; KaF: Karakorum; CF: Chaman; MFT: Main Frontal Thrust; JF : Jiali), sutures (yellow TS Tsangpo; pink BS Bangong; blue JS Jinsha) and subduction trench (thick black lines with triangle; from Hall et al., 2008).

Figure 2 : (a) Horizontal sections at different depths of the P-waves global tomography model of A. Villasenor (described in Replumaz et al., 2010b). Pink dashed lines: cross-sections of figure 3. (b) contour of the positive anomalies interpreted as slabs; TH is related to the Tethyan oceanic slab; IN, HK, BU and AN to Indian continental slabs; CR to the Indian craton; AS, PA and TI to Asian continental slabs. Green lines show the geometry of continental India after the breakoff of the oceanic root (Negredo et al., 2007), rotated at different time using the poles given by Patriat and Achache (1984).

Figure 3 : tomographic north-south cross-sections (see figure 2 for localisation) showing geometric lateral variations and relative position at depth of anomalies TH, related to the Tethyan oceanic slab, IN and HK to the Indian continental slabs, AS and TI to Asian continental slabs, CR to the Indian craton. Arrows indicate sutures (yellow TS Tsangpo; pink BS Bangong; blue JS Jinsha). A/ Dotted orange line shows the equivalent horizontal extend of the vertical Indian slab related to anomaly HK.

Figure 4 : a/ The positive anomaly TH below 1000km depth is related to the Tethys slab detached from the Indian continent. It shows the position of the trench at the onset of collision and draws the geometry of the northern boundary of India at the time of break-off. The length of the Indian continent has been constrained by the length of the Indian slab (dashed lines) as it is present-day subducting beneath the Hindu Kush (figure 3A). It is very similar to the size of the Indian continent deduced from its position in between Australia and Antartica (Gibbons et al., 2012; Zahirovic et al., 2011). Using the paleo-position of India by Patriat and Achache (1984), a breakoff at 45 Ma fits the north of the anomaly (red contour), while a breakoff at 50Ma fits the south of the anomaly (pink contour) (Negredo et al., 2007).

b/ The TH anomaly (dotted blue contour) also shows the southern Asian margin geometry at the onset of collision. Such margin is in agreement with the Asian tectonics reconstruction of Replumaz and Tapponnier (2003) showing a linear margin (pink contour), not with reconstructions showing an asymmetric margin (light blue contour) (Royden et al., 2008), or a margin with a residual indentation (green contour) (van Hinsbergen et al., 2011).

Figure 5 : Subduction processes occurring during the collision, since the breakoff of the Tethyan oceanic root (TH anomaly) at ~45 Ma. The Asian lithosphere subducted soon after the OCT breakoff along a wide part of the collision front (AS anomaly). **A/** To the west, India resumes subducting far north of the Tethys trench, beneath the Hindu Kush (HK anomaly), late in the collision history at ~10 Ma. **B/** It faces the Asian lithosphere, subducting beneath Pamir (PA anomaly). **C/** In the middle of the collision zone, India resumes subducting soon after the breakoff (IN anomaly) between 40 and 30 Ma, which ends by a second breakoff ending at ~15Ma. **D/** To the east, the northern margin of India is extruded eastward (anomalies BU and AN, not visible at these longitudes, see figure 2). Asian lithosphere underthrusts Tibet (TI anomaly).

Figure 6 : (left) successive steps of tectonics reconstruction, showing the position of India and Indochina constrain by paleomagnetic anomalies, the evolution of fault pattern and of the suture positions (pink: Bangong suture, blue: Jinsha suture, yellow: Tsangpo suture), the northern limit of Indian lithosphere (thick black line, with triangle for subduction, dashed for breakoff and solid for underthrusting) and Asian subductions (thick black line with triangle). (right) corresponding P-waves global tomographic sections at different depth, showing the positions of the slabs with time and space.

Figure 7 : (a) area at the onset of indentation of India (dark orange) and Asia (light grey) to be compare to (b) the present-day area of Himalaya (light orange) and Asia (dark grey). (c) The present-day crustal mass (volume measured between the Moho and the topography surface, adding the volume of erosion, crustal mass estimates using a simplified depth/density profile, see Replumaz et al., 2010c for more details) spreads over the present-day area gives a present-day mean thickness of 65 km for the Himalaya and 44 km for Asia. The same mass spreads over the initial area of the blocks, gives a thickness of ~19 km for India and 33 for

Asia. This estimates the thickness that has been stored within the thickened crust or redistributed by extrusion, but spared from subduction. It shows that about half of the Indian crust has been recycled in the mantle and only a negligible amount of the Asian one.

Figure 8 : Numerical models of complete (left) and partial (right) breakoff at OCT. Top: frontal view of the breakoff evolution through time. Middle: top view of the margin geometry evolution. Bottom: top view of stress generated by the breakoff (white dotted line) in the upper plate.

Figure 9 : 3D view of the density model. Velocity field at the trench (black to white arrows depending on the y component) shows horizontal motion to the side of the model, related to underthrusting of the upper plate, and vertical motion in the middle, related to steep subduction, whatever the size of the breakoff, complete (top) or partial (bottom). Stream lines on the middle symmetric plane shows two independant convective cells on both part of the slab, even with a complete breakoff. It shows that the mantle flow is sufficient to pull the continental plate down and drive continental subduction.

Figure 10 : Tomographic section at 52.5 km depth showing a prominent positive anomaly below the Indian craton (CR), which prolongates below the Southern Tibetan Plateau. It corresponds to the present-day northern boundary of the Indian lithosphere (thick green line) below Asia. To the west it stops where the Indian continent subducts beneath the Hindu Kush, beneath Pamir it reaches the Asian slab subducting to the south, beneath Western Tibet it reaches the Tarim basin, and to the east it reaches only the Tsangpo suture (yelow line). The area comprised between the Tsangpo suture and the northern boundary of the Indian lithosphere represents the amount of Indian underthrusting beneath Asia. The area comprised between the northern boundary of the Indian lithosphere and the contour of the India continent at the time of the break-off rotated to its present-day position (dashed green line, in agreement with the length of the Indian slab beneath the Hindu Kush rotated to horizontal shown by the orange dotted line as on figure 3A) provides an estimate of the total amount of Indian lithosphere involves in the indentation process consumed by subduction or extrusion.

Figure 11 : (a) Geometry and position of the slabs observed in the mantle as deep positive tomographic anomalies, projected on the earth surface. (b) The area comprised between the Indian northern boundary at the time of the break-off (in light orange) and the present-day northern boundary of underthrusting India (green line), provides an estimate of the total amount of Indian lithosphere involved in the indentation process. The anomalies HK, IN, BU and AN (black dashed lines) have been interpreted as the result of successive continental subduction episodes, which successively removed a portion of the northern margin of Indian lithosphere. This balance shows that the continental subduction, the extrusion and underthrusting processes accommodated the entire lithosphere of the northern Indian margin since the onset of indentation. On the contrary, the anomalies PA and AS (pink dashed lines) removed a limited amount of the Asian lithosphere, which could not account for the entire Asian lithosphere north of the Tsangpo suture.

Figure 12 : (left) 3D view of the successive events occurring along the northern margin of India showing the complex long term evolution of the system. (middle) stress generated in the upper plate by partial or complete breakoff. (right) Fault pattern reconstructed for Asian at different time steps. Our models show that successive Indian slab breakoff episodes have resulted in successive localized stress pulses which provide the conditions for the formation of Central Asian intra-continental faults. Transient coupling gradients at the trench caused by the breakoff events during India-Asia convergence offer an explanation for episodic nucleation of lithospheric faults within the Asian continent and their link to deep processes.

Anne Replumaz is a CNRS Senior Researcher at ISTerre (Institut des Sciences de la Terre, Grenoble, France). She received her PhD at IPGP (Institut de Physique du Globe de Paris, France). She has dedicated is career on using quantitative field data at a pertinent scale to constrain the processes driving the continental deformation during the India/Asia collision. She has quantified the slip-rate of faults, used to made a complete reconstruction in time and space of the motion along faults, which was pertinent to compare the crustal deformation with the mantle tomographic positive anomalies, and to constrain analog and numerical models of continental deformation. She has published her results in international journals of broad impact.

Fabio Capitanio is a Senior Lecturer at Monash University, Melbourne, Australia. He received his MSc from Roma Tre University, Italy, and the PhD from ETH, Switzerland. His research fields include tectonics, geophysics and geodynamics, with a focus on the mechanics of the convergent margins and continental tectonics. He has published many publications in international journals of broad impact. He is the recipient of the 2012 Jason Morgan Early Career Award by the American Geophysical Union, and the 2013 Discovery Early Career Award by the Australian Research Council.

Stéphane Guillot, Director of Research at CNRS of Grenoble, is a specialist of Himalayan geology. He currently works in active convergent zones (Asia, Alps, Oman). He published more than 100 publications and participated to the publication of book dedicated to Himalaya and Tibet geodynamic evolution (Mascle G., Pêcher A. and Guillot S., 2012- The Himalaya-Tibet Collision. Book series, Geological Society of Nepal).

Ana-Maria Negredo-Moreno is Professor of Geophysics at the University of Madrid (Spain). She is an internationally recognized expert on numerical modeling with an emphasis on subduction processes.

Antonio Villaseñor is a staff scientist at the Spanish National Research Council's Institute of Earth Sciences Jaume Almera (ICTJA-CSIC). He received his undergraduate training and Ph.D. in Physics (1995) from the University of Barcelona, Spain. After postdoctoral stays at the U.S. Geological Survey (Golden, USA), University of Colorado (Boulder, USA) and University of Utrecht (The Netherlands) he joined ICTJA-CSIC in 2004. His main research interests include the study of global instrumental seismicity and earthquake tomography. He has studied volcanic systems using local earthquake travel times, the Eurasian continent using surface waves from earthquakes and correlations of ambient noise, and the whole Earth's mantle using teleismic travel times. Currently he is also involved in the study of induced seismicity caused by fluid injection.

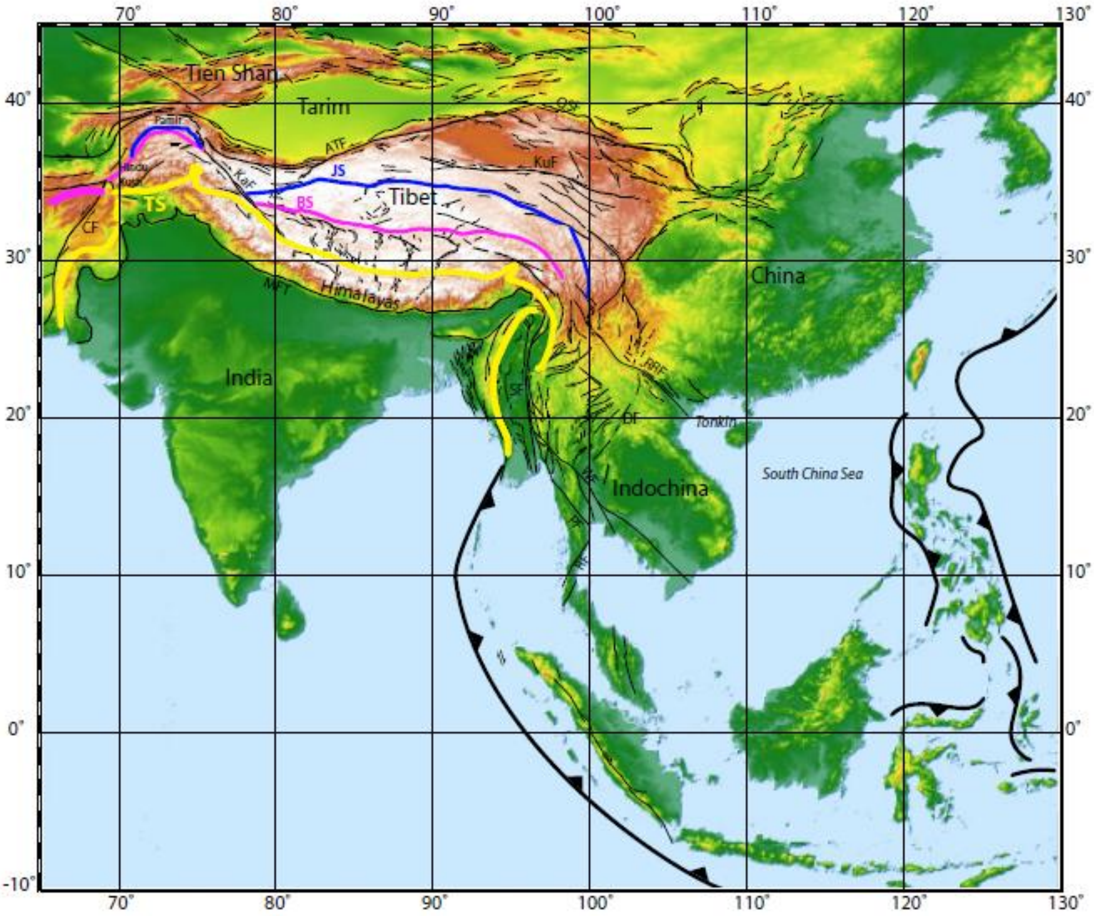
Tien Shan
Tarim
Tibet
China
India
Indochina
Himalayas
South China Sea
Tonkin
Pamir
JS
BS
TS
ATF
KuF
KaF
MFT
CF
70°
80°
90°
100°
110°
120°
130°
40°
30°
20°
10°
0°
-10°

Figure 1

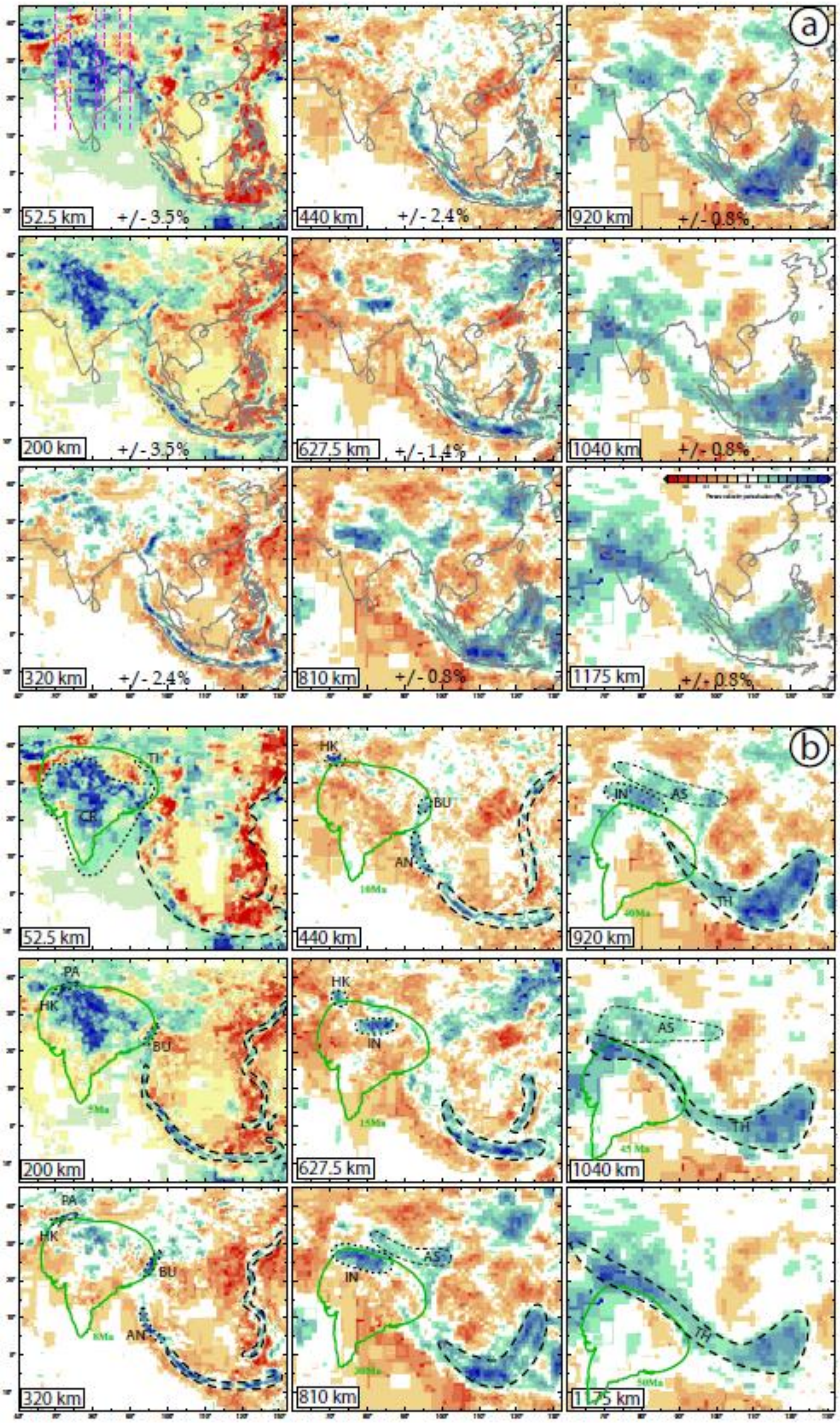
a
52.5 km
+/- 3.5%
440 km
+/- 2.4%
920 km
+/- 0.8%
200 km
+/- 3.5%
627.5 km
+/- 1.4%
1040 km
+/- 0.8%
320 km
+/- 2.4%
810 km
+/- 0.8%
1175 km
+/- 0.8%
b
TI
CR
HK
BU
AN
IN
AS
TH
PA

Figure 2

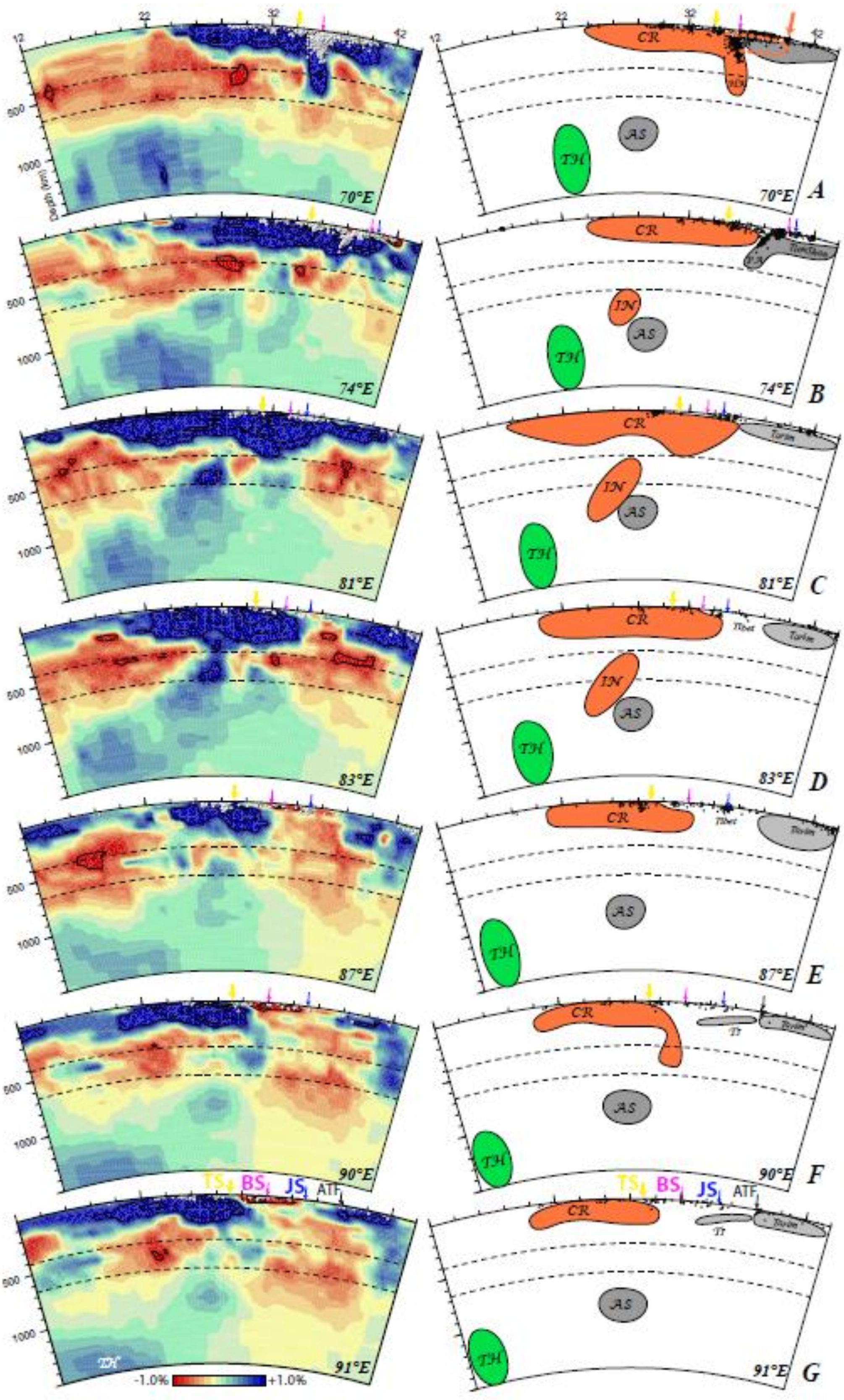
70°E
A
74°E
B
81°E
C
83°E
D
87°E
E
90°E
F
91°E
G
CR
AS
TH
IN
Tarim
Tibet
TS
BS
JS
ATF
-1.0%
+1.0%
500
1000
12
22
32
42

Figure 3

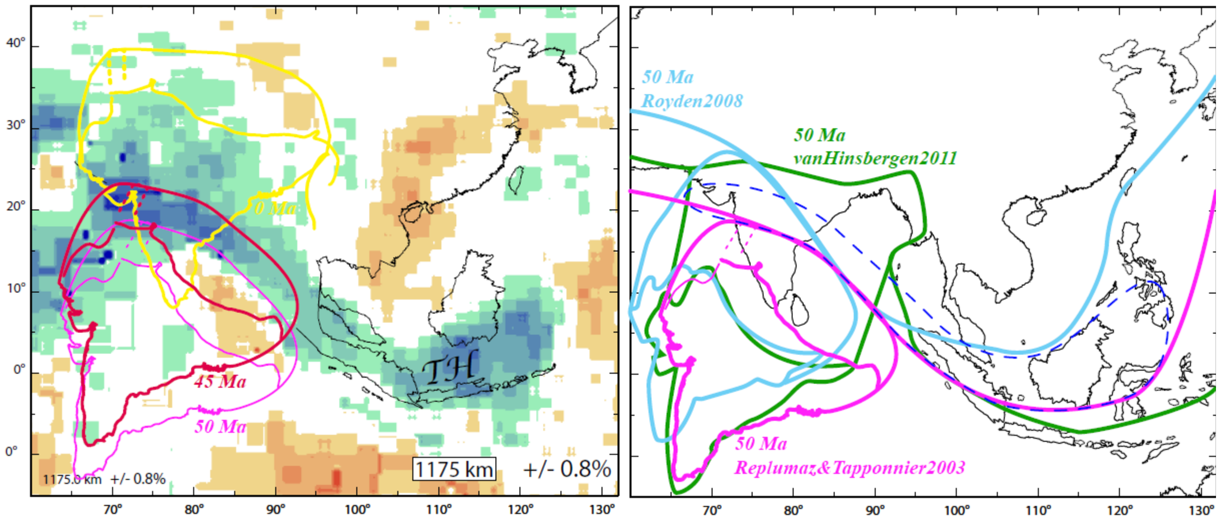
40°
30°
20°
10°
0°
0°
0 Ma
45 Ma
50 Ma
TH
1175.0 km +/- 0.8%
1175 km
+/- 0.8%
70°
80°
90°
100°
110°
120°
130°
50 Ma
Royden2008
50 Ma
vanHinsbergen2011
50 Ma
Replumaz&Tapponnier2003

Figure 4

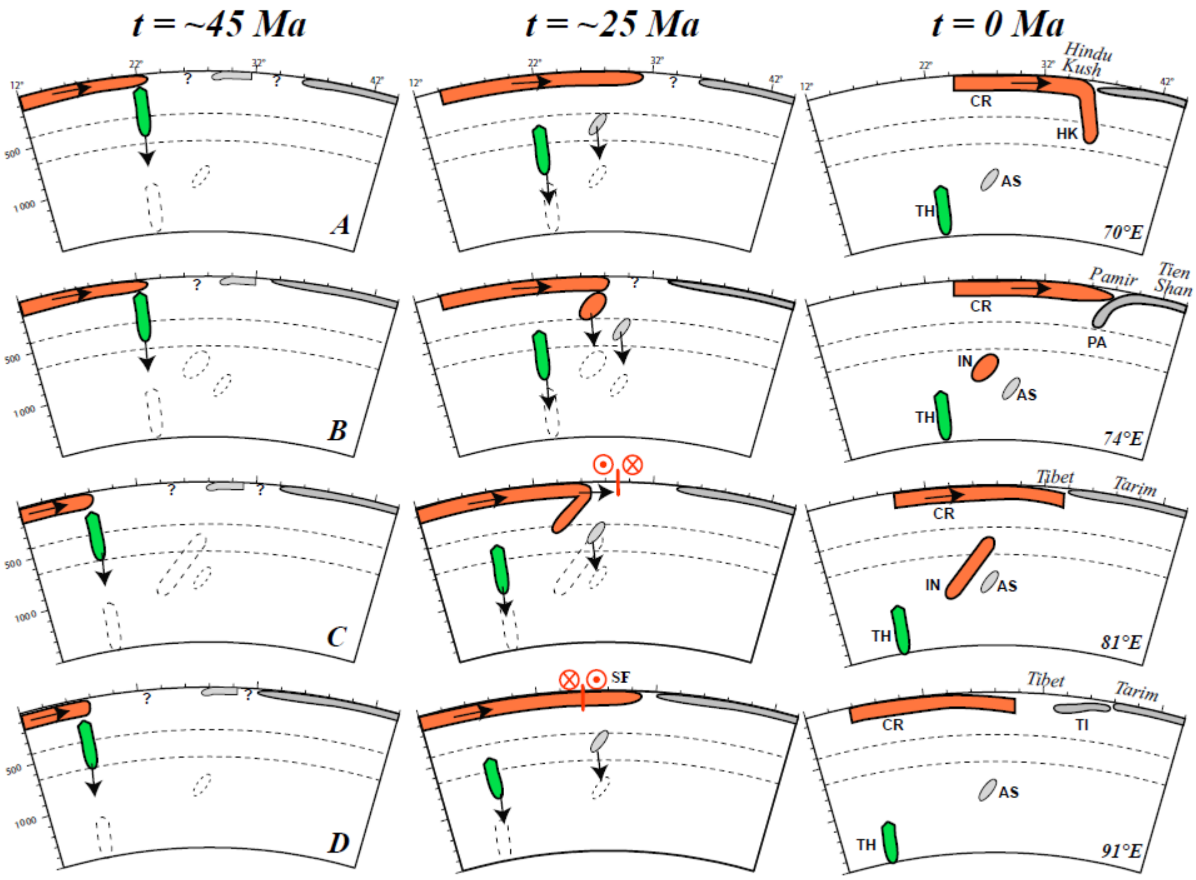
t = ~45 Ma
t = ~25 Ma
t = 0 Ma
Hindu Kush
CR
HK
AS
TH
70°E
A
Pamir
Tien Shan
PA
IN
74°E
B
Tibet
Tarim
81°E
C
SF
TI
91°E
D
500
1000

Figure 5

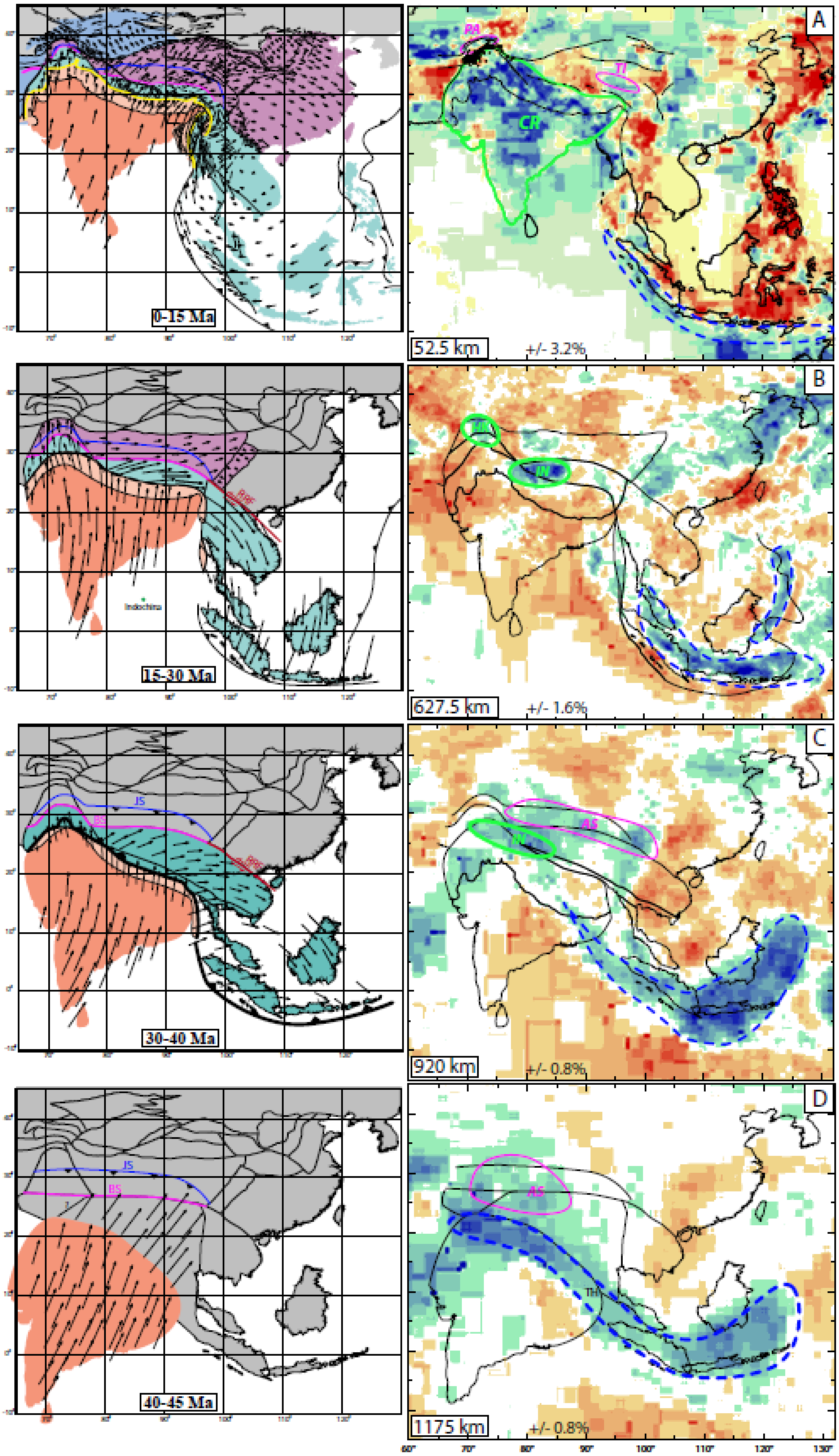
0-15 Ma
15-30 Ma
30-40 Ma
40-45 Ma
Indochina
JS
BS
RRF
A
B
C
D
PA
TI
CR
HI
IN
AS
52.5 km
+/- 3.2%
627.5 km
+/- 1.6%
920 km
+/- 0.8%
1175 km
+/- 0.8%

Figure 6

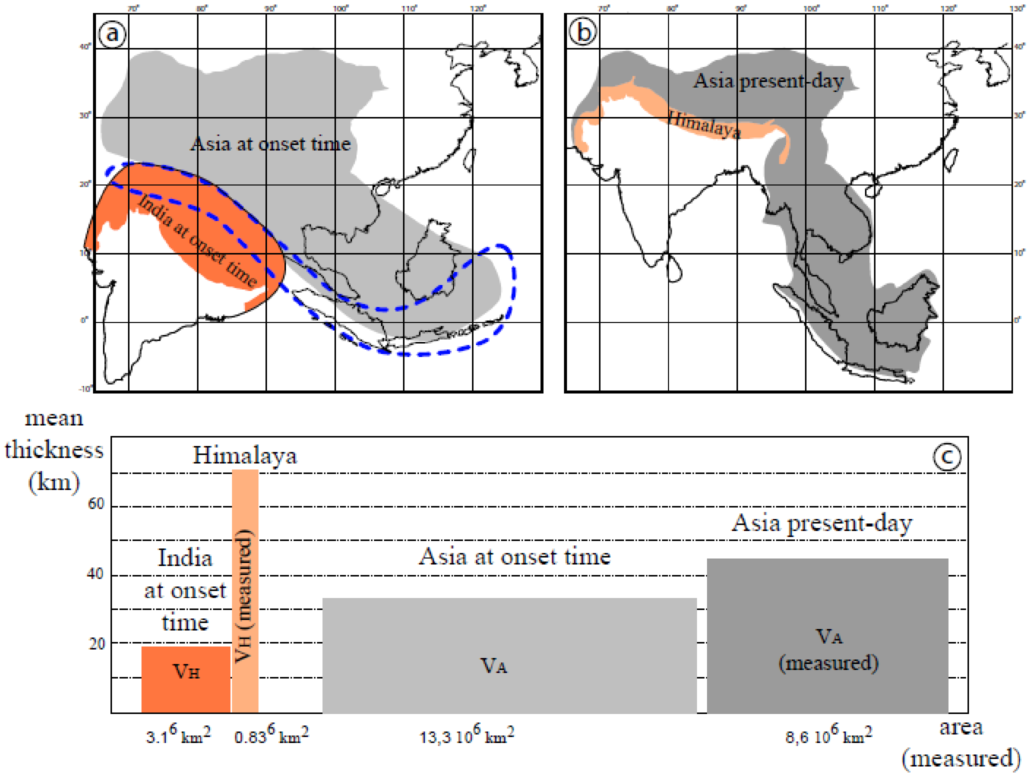
a
Asia at onset time
India at onset time
b
Asia present-day
Himalaya
mean
thickness
(km)
60
40
20
c
Himalaya
Asia present-day
India
at onset
time
VH (measured)
Asia at onset time
VH
VA
VA
(measured)
3.1⁶ km²
0.83⁶ km²
13,3 10⁶ km²
8,6 10⁶ km²
area
(measured)

Figure 7

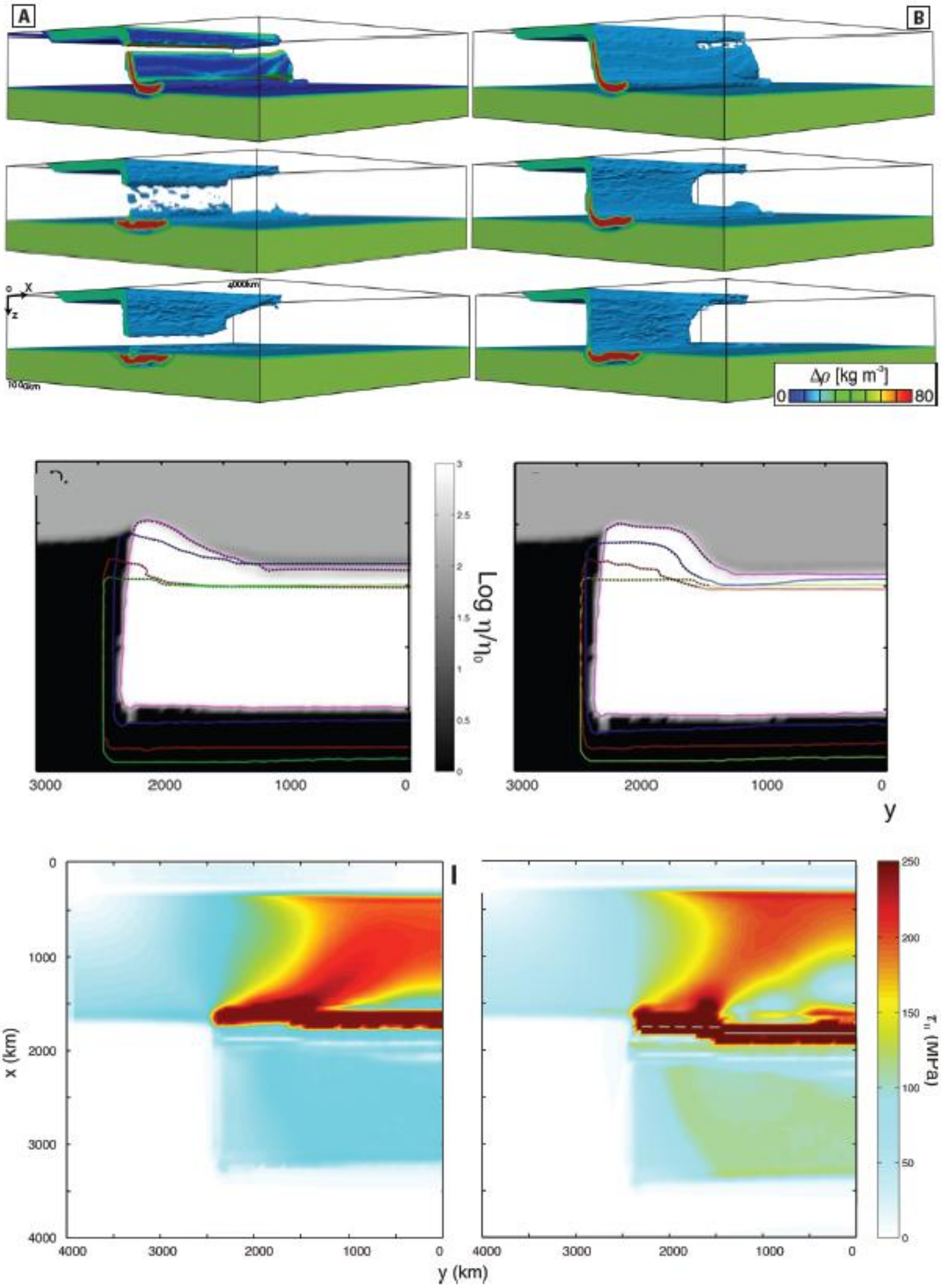
A
B
X
z
4000km
1000km
Δρ [kg m^-3]
0
80
3000
2000
1000
0
y
Log η/η0
x (km)
y (km)
4000
τII (MPa)
250
200
150
100
50

Figure 8

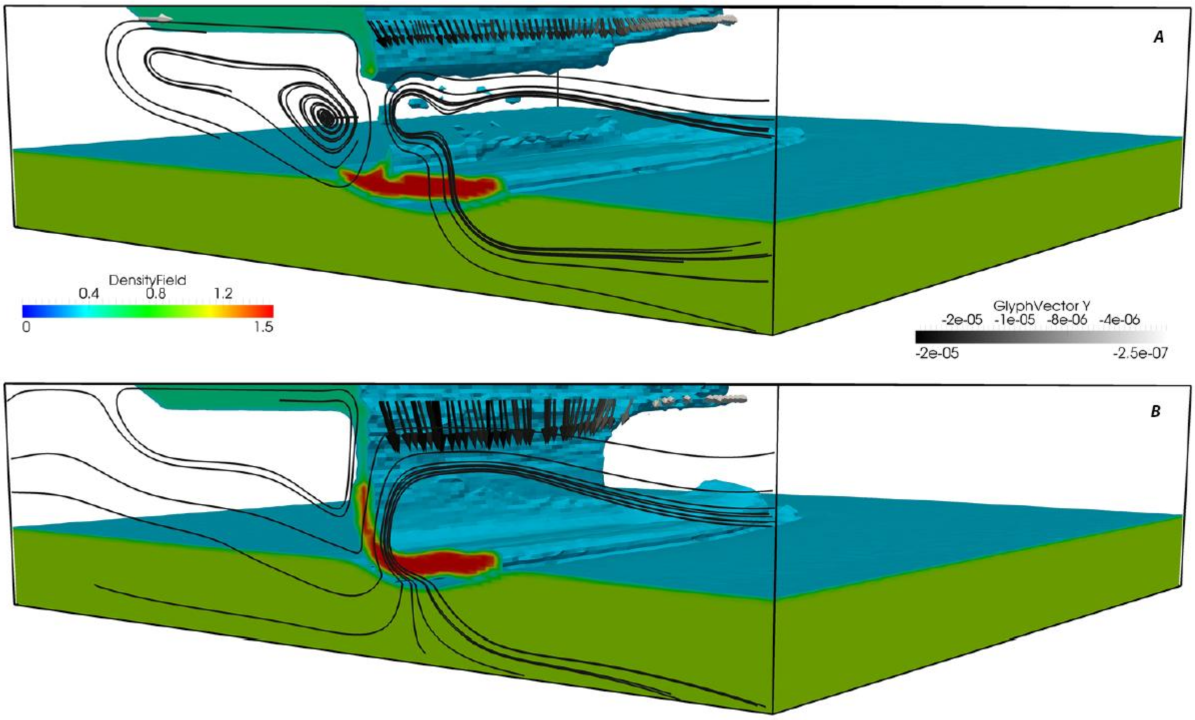
A
B
DensityField
0.4
0.8
1.2
0
1.5
GlyphVector Y
-2e-05
-1e-05
-8e-06
-4e-06
-2e-05
-2.5e-07

Figure 9

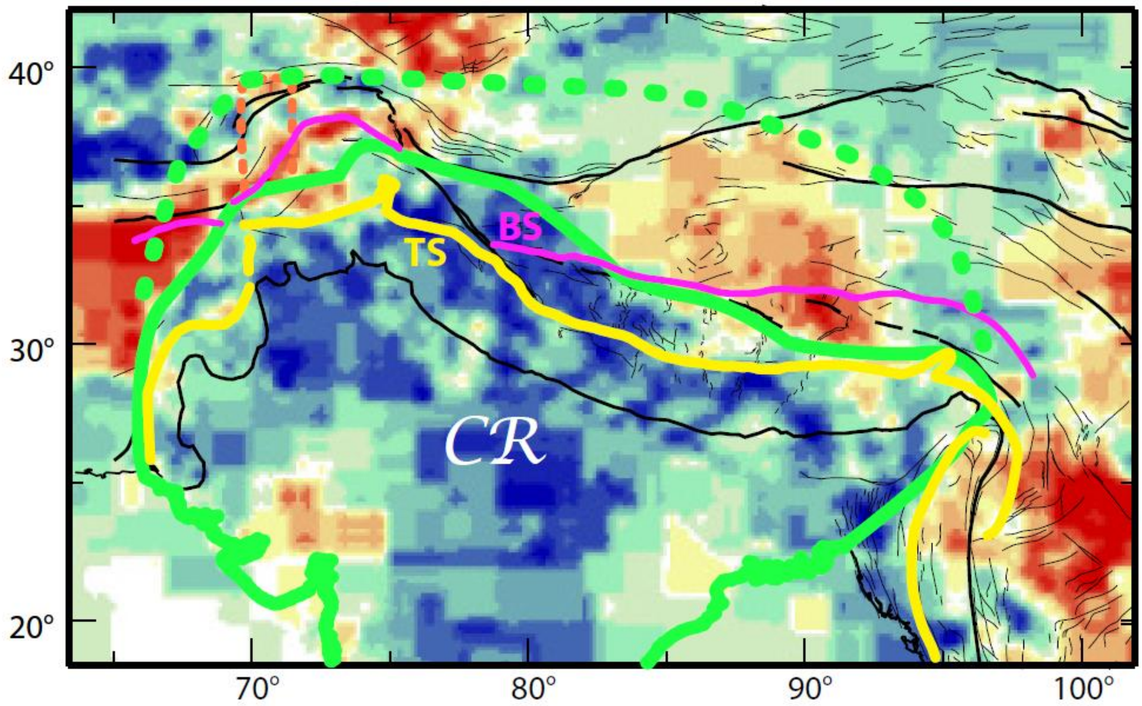

Figure 10

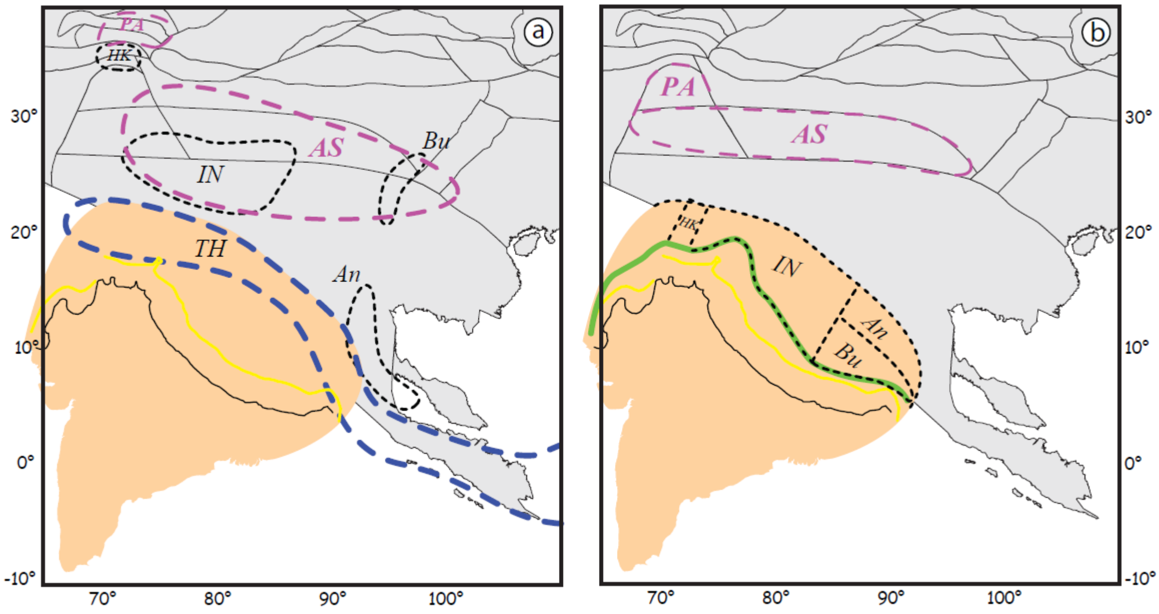
a
PA
HK
AS
IN
Bu
TH
An
30°
20°
10°
0°
-10°
70°
80°
90°
100°
b
PA
AS
HK
IN
An
Bu
30°
20°
10°
0°
-10°
70°
80°
90°
100°

Figure 11

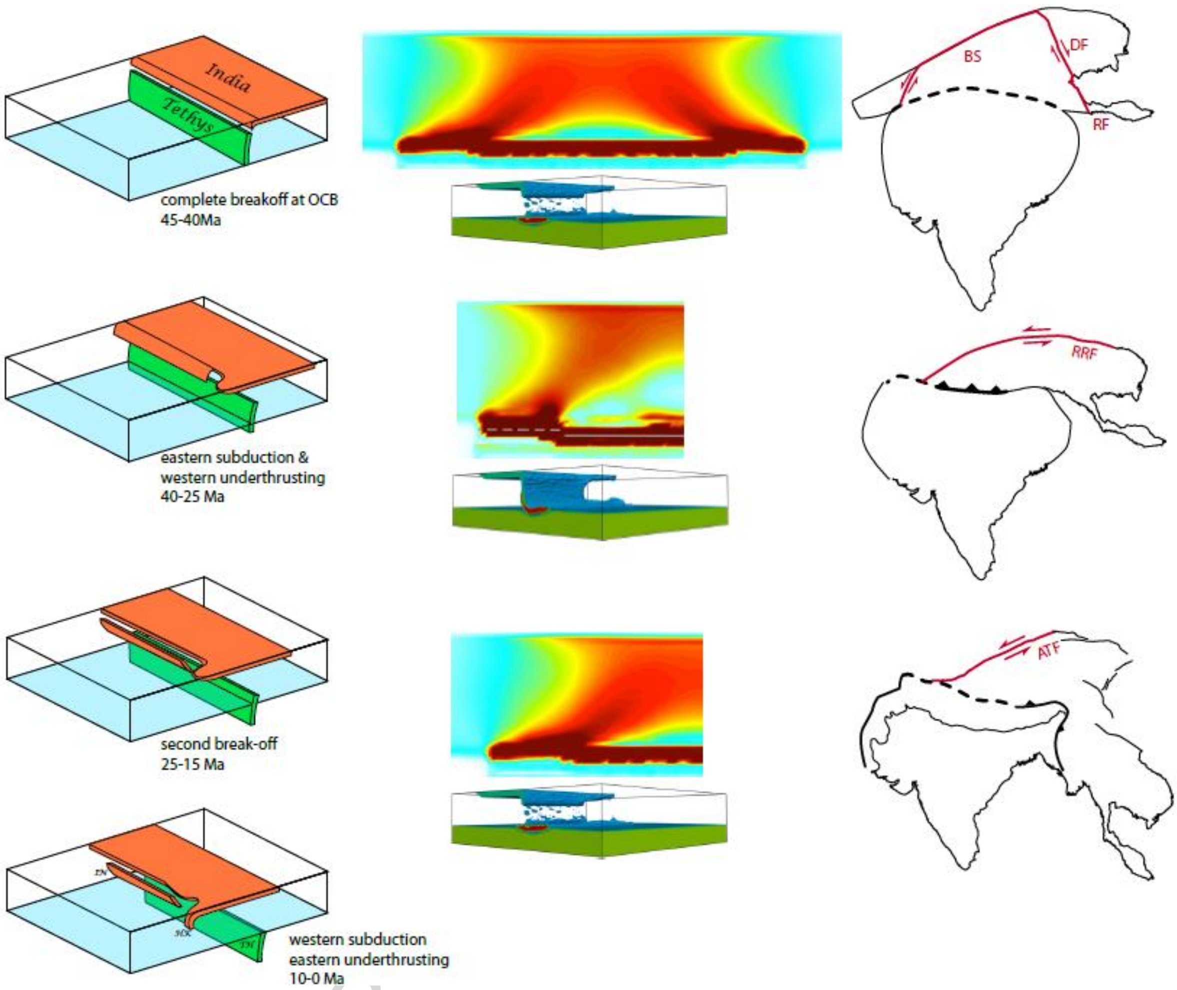
India
Tethys
complete breakoff at OCB
45-40Ma
eastern subduction &
western underthrusting
40-25 Ma
second break-off
25-15 Ma
western subduction
eastern underthrusting
10-0 Ma
BS
DF
RF
RRF
ATF

Figure 12

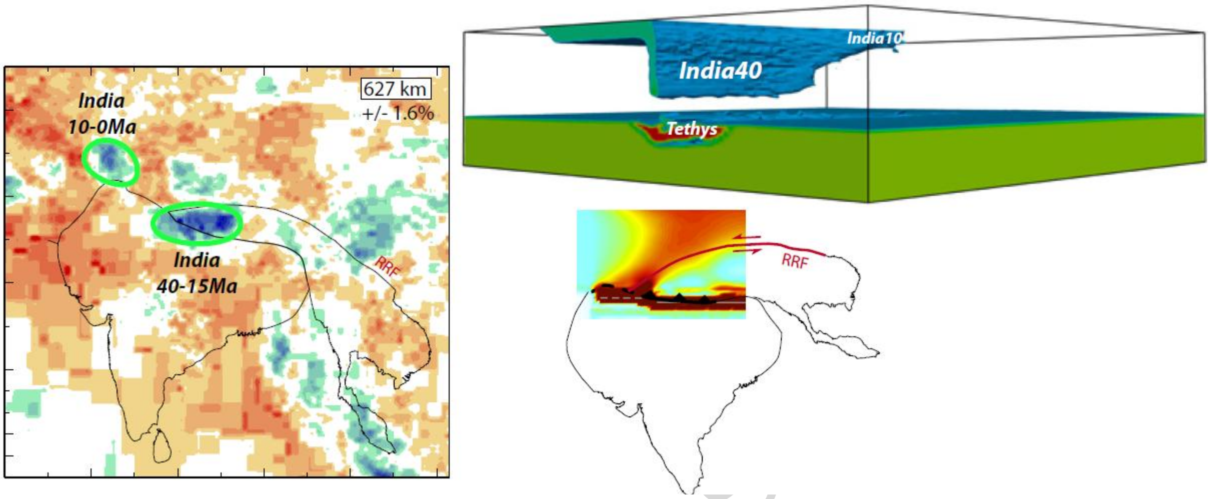

Graphical abstract

Highlights

Global tomography evidences Indian continent subduction and breakoff

After complete breakoff at the OCT, Indian continent subduction resumes

Mantle flow generates by oceanic subduction drags the Indian continent in the mantle

Indian slab breakoff generated localized stress pulses in Asian continent